No 727481 RESERVE

D3.5 v1.0

Specification for an On-Line System Level Monitoring System

The research leading to these results has received funding from the European Union's Horizon 2020 Research and Innovation Programme, under Grant Agreement no 727481.

Project Name	RESERVE
Contractual Delivery Date:	30.09.2018
Actual Delivery Date:	29.09.2018
Contributors:	RWTH, UCD, WIT, EDD, ESB, GH
Workpackage:	WP-3 – Voltage Control
Security:	PU
Nature:	R
Version:	1.0
Total number of pages:	51

Abstract:

This deliverable presents the system level monitoring concept of the two-fold solution developed in RESERVE for control and monitoring of low voltage distribution grids. In SV_A, a novel and generalised virtual output impedance framework is defined and specified which allows the DSO operator to modify the inverters dynamic behaviour. In SV_B, a hierarchical active voltage management algorithm is proposed in which the local solve the voltage problems and the system level control maintains accuracy in the local system identification. Specification for system level integration is defined for both voltage control scenarios from both power and ICT perspective. Network code implications of the new technique and planned simulation/field trial activities to validate network codes are reported.

Keyword list:

Voltage stability, Stability monitoring, Dynamic voltage stability monitoring, Virtual output impedance, Volt-var curve.

Executive Summary

This deliverable presents the system level monitoring concept of the two-fold solution developed in RESERVE. On the one hand, there is Dynamic Voltage Stability Monitoring (DVSM) also known as SV_A which handles dynamic voltage stability issues and Active Voltage Management (AVM) also known as SV_B for steady-state voltage control. Specifications for system-level integration from both power and ICT perspective are provided.

Review of various Virtual Output Impedance (VOI) and active damping techniques was performed. A gap was identified in the way VOI controllers were defined. Many of the methods do not take the time-varying nature of the grid impedance. Few of the methods that do consider grid impedance measurement do not have a generalised design procedure for the design of VOI controllers.

This deliverable addresses the above-mentioned gap by presenting a generalised framework for the synthesis of a class of robust VOI controllers based on the real-time grid impedance measurements. Parameters of the weighting function can be used to modify the inverter output impedance. Validation of the proposed technique is performed in both time and frequency domain in offline simulations.

The system-level implementation of the SV_A technique was analysed. Particularly, the placement of the WSI tool in the system. The first possibility is the inverter hosting the WSI tool locally. The controller hardware needs to be computationally powerful whereas the communication data volume is low. The second possibility is where the WSI tool is implemented centrally in SSAU. Here, the communication data volume is high although the controller of the inverter can be cheap.

In Chapter 3, a hierarchical active voltage management algorithm is proposed in which the local controllers try to solve the voltage problems and the system level control keeps the local system identification results as accurate as possible. Under such setup, the control strategies are quickly extracted by the local control systems to adaptively meet the real-time requirements of active voltage management in the current low voltage distribution systems and the system model applied in the local control systems is kept up-to-date by the system level control to mitigate the potential errors. After utilizing the VVCs and finding the new settings of each inverter, it might be possible that more corrections are required according to the new set of PCC voltages. A supervised closed-loop control is proposed here to achieve a near optimal reactive power dispatch between the system controllable devices for better voltage control. Regarding this supervised control, the other task of the system level control is to initiate the control process to reach a balanced state. This chapter also provides insight on how to consider different objectives simultaneously for AVM which leads to a higher exploitation of the system control capacity. The simulation results achieved in Chapter 3 demonstrates the impact of system level monitoring concept on **Active Voltage Management** technique. Furthermore, this chapter provides detail of the execution of the VVC from an ICT perspective, it includes the building of software components built to receive the curve, store it and calculate the reactive power set point that is then sent to the relevant device(s). These software components have been built in a modular way to enable their effective deployment in all the ICT system architectures and infrastructures detailed in D3.6. This means components charged with the receipt, storage, and execution of the VVC, while inter-dependant, can be individually deployed in various locations throughout the system.

Authors

Partner	Name	e-mail
RWTH		
	Sriram Karthik Gurumurthy	Sgurumurthy@eonerc.rwth-aachen.de
	Antonello Monti	Amonti@eonerc.rwth-aachen.de
UCD		
	Alireza Nouri	alireza.nouri@ucd.ie
	Alireza Soroudi	alireza.soroudi@ucd.ie
	Andrew Kaene	andrew.keane@ucd.ie
WIT		
	David Ryan	dryan@tssg.org
	Miguel Ponce De Leon	miguelpdl@tssg.org
	Niall Grant	ngrant@tssg.org
EDD		
	Steffen Bretzke	steffen.bretzke@ericsson.com
ESB		
	Ronan Murphy	ronan.murphy@esb.ie
	Jonathan Sandham	jonathan.sandham@esb.ie
GH		
	Artur Löwen	aloewen@gridhound.de

Table of Contents

1. Introduction

This deliverable summarises the activities of **Task 3.5** of WP3.

1.1 Task 3.5

Within the context of WP3, the challenges posed by distribution grids with increasing RES penetration were studied. Dynamic Voltage Stability Monitoring (DVSM) and Active Voltage Management (AVM) scenarios were developed during the first year of the project. Since LV power systems are the focus in WP3, we envision system level strategies defined and specified for the applicability of the proposed scenarios in the future LV grids. This deliverable covers the specification of system level monitoring techniques of the two scenarios SV_A and SV_B. The ICT implications of the new techniques are also addressed. These new techniques require new network codes or modification in existing network codes and the preparation of field trials in relation to the validation of the proposed network codes are also addressed in this deliverable. This deliverable summarises the activities and work done to achieve the milestone **MS 8** which is on the definition and specification of system level monitoring concept.

1.2 Objectives of the deliverable

The objectives of the deliverables are as follows:

- Specify system level monitoring concept for SV_A Dynamic Voltage Stability Monitoring (DVSM)
- Specify system level monitoring concept for SV_B Active Voltage Monitoring (AVM)
- ICT implications of the proposed system level montioring conepts
- Reporting of field trials and real-time simulations in relation to network code validation

1.3 Outline of the Deliverable

The outline of the deliverable is as follows:

- Chapter 2 - System level monitoring concept of SV_A.
- Chapter 3 - System level monitoring concept of SV_B
- Chapter 4 - Activities undertaken in preparation of field trials for the validation of the two scenarios: both from a concept validation standpoint and network code validation
- Chapter 5 - Overall conclusion and future work

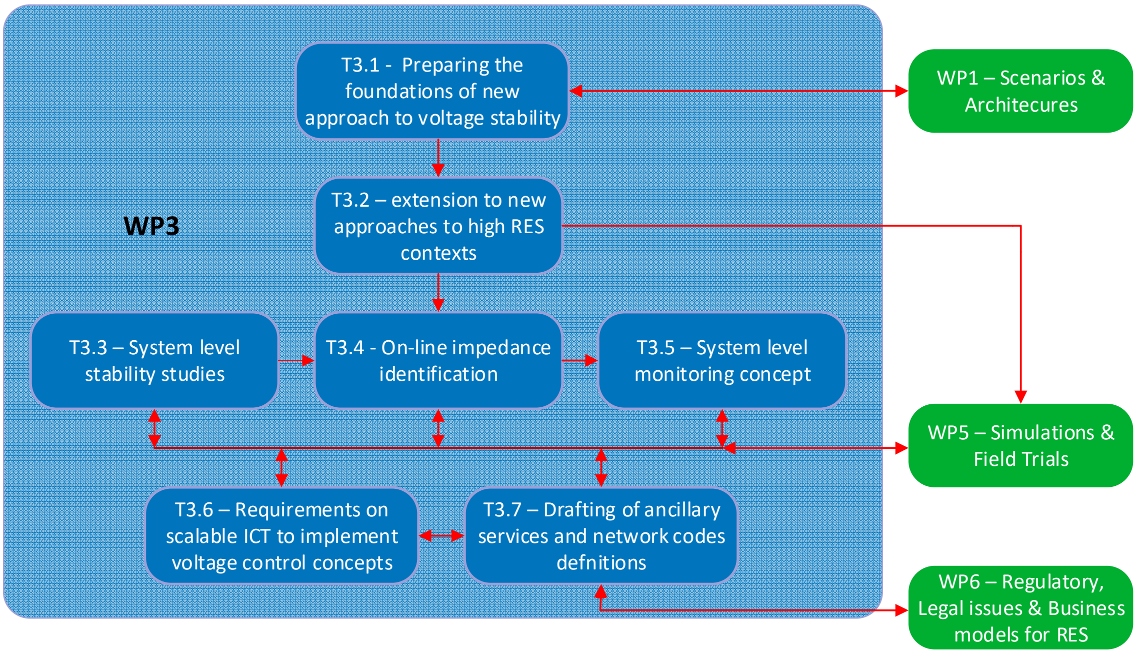

Figure 1-1 Relations between Tasks in WP3 and other Work Packages

1.4 How to Read this Document

The reader is expected to go through deliverables **D3.3** and **D3.4** before reading this document. This deliverable uses the stability monitoring algorithm from deliverable **D3.3** and uses the WSI concept defined in deliverable **D3.4**.

2. System level monitoring concept based on SV_A: Dynamic Voltage Stability Monitoring (DVSM) technique

Dynamic Voltage Stability Monitoring (DVSM) technique or SV_A is a three-step process. The first step is where the Secondary Substation Automation Unit (SSAU) commands the inverter to inject noise and measurement. The second step is where the inverter uses its local measurements and non-invasive Wideband System Identification (WSI) to identify the grid impedance model and sends it to the SSAU. The inverter also sends its output impedance which is known locally to the controller of the inverter. The last step is on the calculation of dynamic stability margins and synthesis of virtual output impedance (VOI). The stability criterion for calculating the stability margins for power-electronic systems is covered in D3.2 and its extensions were carried out in D3.3. The novel generalised design procedure that is developed in RESERVE is reported in this deliverable. This final step closes the loop on a system level, since the SSAU send back the VOI control coefficients back to the RES inverter to modify its behaviour; in this case, modifying its output impedance.

A major change is taking place in the power sector with the increased penetration of renewable energy sources (RES) in the grid. Tightly coupled parallel inverters in low voltage AC (LVAC) grids are known to cause parallel resonance phenomenon which poses a threat to voltage instability [1]–[3]. In general, virtual output impedance (VOI) control solutions are proposed for solving power sharing problems and harmonic instability problems [2], [4]–[7]. VOI loops are used to shape the output impedance of the filter and provide active damping [2], [4], [7], [8]. Recently, a power electronic converter based active grid impedance cancellation technique was proposed [9]. The above-mentioned work involves hardware and there comes under the category of invasive design. However, the proposed method in this paper is non-invasive, meaning that additional hardware is not required and the desired output impedance can be realized through VOI control loops which can be implemented as a digital controller. Another adaptive VOI method which uses real-time grid impedance measurement was proposed in [2], [8]. This method is not suitable to distribution grids due to its assumption of the grid impedance with an inductance. Due to the parallel connection of inverters, the grid impedance at all frequencies within the bandwidth of the controller needs to be considered. Within WP3, we have proposed the WSI based grid impedance measurement which can measure and estimate the grid impedance model for frequencies within the control bandwidth. Therefore, with the inclusion of WSI techniques, one can get a more realistic higher order impedance model [10]. The focus of this deliverable is on the novel procedure for VOI design and on the system level integration of DVSM technique. Details on the WSI tool for grid impedance measurement in covered in *D3.4*.

The goal within SV_A of RESERVE is to achieve voltage stability of grids by actively controlling the output impedance of every power electronic interface. Such an aim requires a generalized design procedure for the synthesis of VOI loop given that the stability at the point of common coupling (PCC) depends on the return ratio matrix of grid impedance and inverters output impedance, as per the generalised Nyquist criterion (GNC) [1], [11]–[14]. The method described in this paper is applicable to all types of power converters. The novelty of this work is the formulation of VOI design as a mixed-sensitivity H-Infinity (H_∞) problem. We would like to emphasize that the mixed-sensitivity H_∞ technique is applied for robustness purposes and to invoke a generalized VOI synthesis paradigm wherein the measured grid impedance can be included into the plant model. It is envisioned that the proposed framework allows DSO networks to vary the RES inverters impedance through 5G communication.

This deliverable addresses the integration of the new power concepts using ICT infrastructure. The possible configurations to implement the WSI tool is discussed and its influence on the requirement of ICT infrastructure is discussed. Furthermore, this deliverable also presents the implications of the novel techniques on network codes and further presents the mapping between planned simulations and network code validation.

2.1 Dynamic Voltage Stability Monitoring (DVSM) algorithm

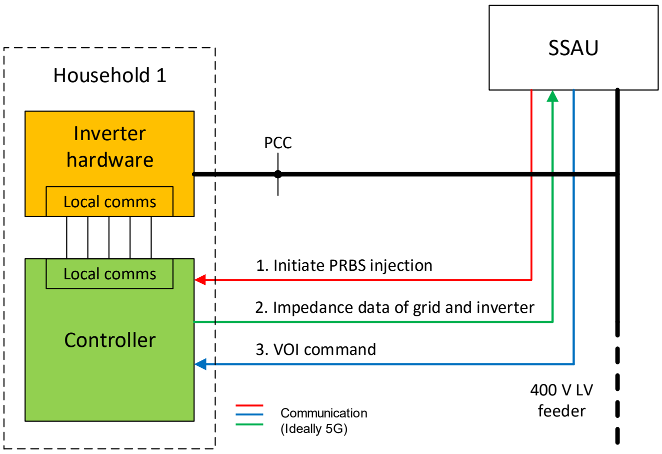

Figure 2-1 DVSM Algorithm (SV_A)

The three-step process of the DVSM technique as shown in Figure 2-1 can be summarised as follows. The first step is the initiate noise injection command from the SSAU to the inverter. Following which the inverter measures the grid impedance. The inverter calculates its output impedance coefficients from the mathematical model which is known to the inverter. In the second step, the inverter hardware communicates the grid impedance data and inverter output impedance data to the SSAU. Following which the SSAU calculates the dynamic stability margins and VOI command. The third step is where the SSAU communicates the VOI command back to the inverter. This completes 1 computation cycle of DVSM for 1 household, let's denote it as t_p seconds. This process is repeated for every household with RES inverter, one at a time. The time period t_p and the number of houses N under a given SSAU is a crucial factor in determining the number of cycles of DVSM (denoted by f_{dvsm}) that can be performed for a given LV distribution system in 1 hour, which is given by (1).

We envision that one cycle of DVSM cycle per household t_p takes about 0.5 to 0.7 seconds. Therefore, on an average considering 500 households under an SSAU, we envision the DVSM cycle for this portion of the distribution grid can be completed in 300 seconds. Therefore, the number of cycles of DVSM for the distribution grid in an hour is roughly 12 to 14 cycles.

$$f_{dvsm} = \frac{3600}{Nt_p} \quad (1)$$

2.1.1 WSI tool implemented locally in RES Inverters

The system level integration of WSI tool when implemented locally in the inverter is shown in Figure 2-2.

- The controller of the inverter has the complete WSI algorithm. This includes the subroutines like PRBS noise generation, extracting the non-parametric impedance and parametric impedance identification.
- The Inverter uses communication to communicate only the identified impedance coefficients. Communication data volume is low.

Considering that the process repeats for an inverter every 5 minutes.

Data Volume/Bandwidth

- Floating point (double precision) – 8 bytes per number
- Number of floating point numbers of grid impedance– 50
- Number of floating point numbers of inverter output impedance– 50
- Number of floating point numbers of VOI command – 50
- Number of inverters (1 Inverter per end-point) – 500

- Kilobytes per second – 8*150*500/(1024*300) = 1.9531 kBytes/s
- Kilobits per second – 15.625 kbits/s

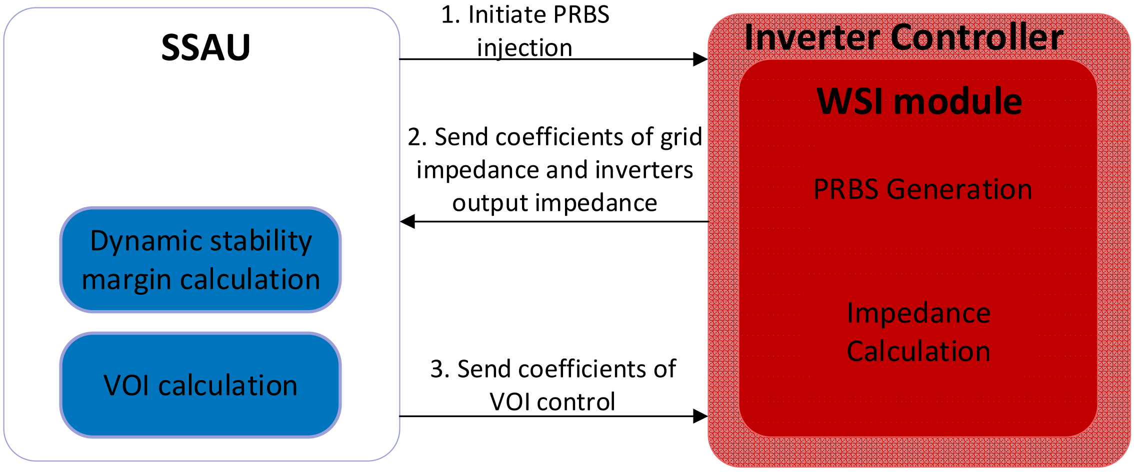

Figure 2-2 System level integration of WSI when locally implemented in inverter

2.1.2 WSI tool implemented in SSAU

The system level integration of WSI tool when implemented in SSAU is shown in Figure 2-3.

- The controller of the inverter has only the PRBS noise generation subroutine.
- The rest of the WSI functionalities such as extracting the non-parametric impedance and parametric impedance identification is performed in SSAU.
- The Inverter uses communication to send voltage and current data measured during the perturbation. Communication data volume is high.

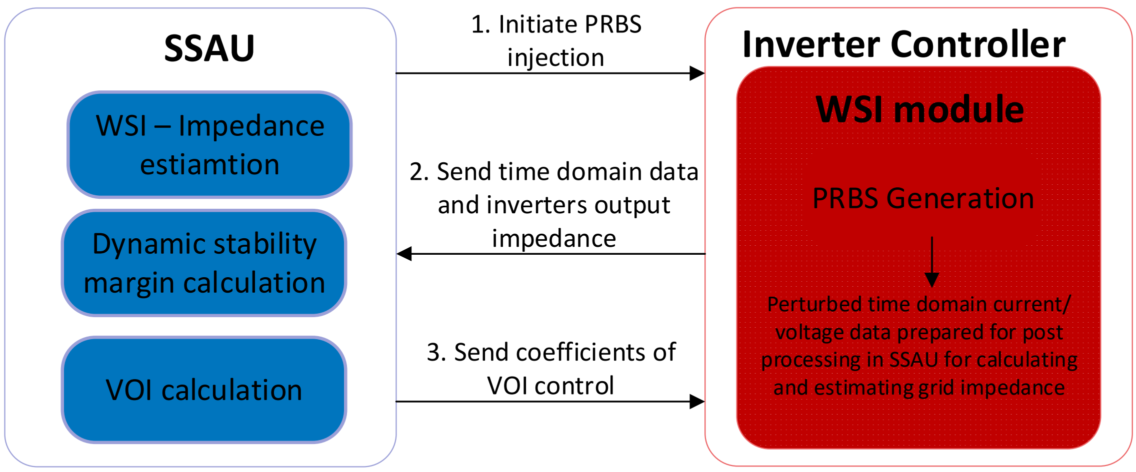

Figure 2-3 System level integration of WSI when implemented in SSAU

Data Volume/Bandwidth

Considering the sampling frequency within the inverter controller of 50 kHz and the number of fundamental cycles (N) of the power system frequency of 50 Hz for which the measurements are recorded, the number of data points can be calculated as: Ns=N*50kHz/50 Hz.

- Floating point (double precision for coefficients) – 8 Bytes per number
- Number of floating point numbers of inverter output impedance – 50

- Number of floating point numbers of VOI command – 50
- Total bytes for all coefficients = 8bytes*(50+50) =800 Bytes
- Time domain data of perturbed signals – 2 Bytes per number
- Number of channels (Vd,Vq,Id,Iq) – 4
- Number of fundamental cycles N -10
- Number of perturbed time domain data Ns - 10*50,000/50 =10,000
- Total bytes of perturbed time domain data – 10,000*4 channels* 2 bytes = 80,000 Bytes
- Overall total data - 80,000 Bytes (from time domain data) + 800 Bytes (Coefficients) = 80,800 Bytes
- Number of inverters (1 Inverter per end-point) – 500
- Kilobytes per second – 80,800*500/(1024*300) = 131.51 kBytes/s
- Kilobits per second – 1052.08 kbits/s

2.2 Proposed VOI control algorithm

The control of the system of the plant, i.e. the inverters plant model and the existing control structure is considered. Typically, inverter manufacturers use cascaded linear controllers. This is because they are easy to design and it is easy to keep track of all the current and voltage variables in the system. This makes it easier to apply saturators on the current and voltage reference signals. The goal in SV_A is to modify this behaviour externally by a DSO operator for example. The proposed design of the VOI considers real-time grid impedance measurements to design the stabilizing VOI loop which can be used to control the dynamics of the inverter control system.

2.2.1 VOI Design for voltage-controlled (VC) inverters

Figure 2-4 shows the control block diagram of the VC inverter. VC inverters have the objective of regulating the output voltage. PV converters are currently used as current-controlled (CC) inverters in distribution grids. A CC inverter acts like a PQ source from a classical power system standpoint. The reactive power (Q) reference does not change dynamically although a Q-V droop such as Volt-var curve could exist for steady-state regulation. A VC inverter on the other hand converters a power reference into a voltage reference and tried to regulate the output voltage based on the active power set point (P). A VC inverter behaves like a PV bus from a classical power system standpoint. Thus, the reactive power Q can be instantaneously controlled (dynamically controlled) according to the output voltage. Futuristic grids will consider such configurations of inverter control for maximising grid-support. We intend to be a step ahead and derive the VOI formulation for VC inverter. In Figure 2-4, the block represented in green Y_{voi}, represents the VOI control block. Note that it tries to modify the reference coming from the outer voltage loop. The measured current $i_{L,dq}$ can be alternatively represented by the ratio of output voltage and the grid impedance. In *D3.4*, a WSI method for identifying the grid impedance parametrically was presented.

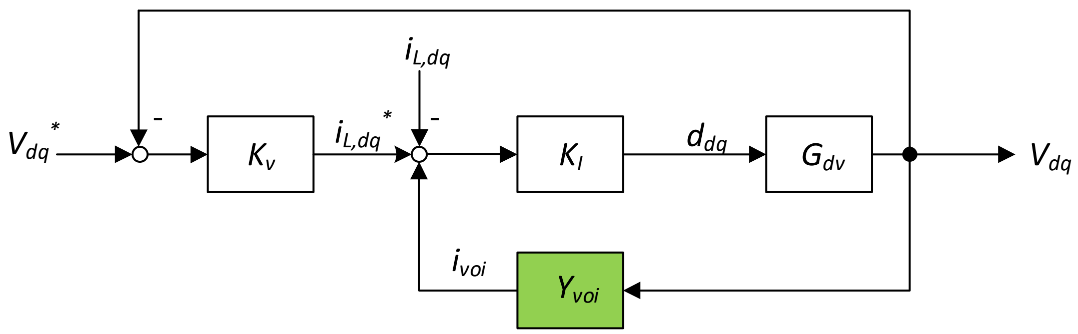

Figure 2-4 VOI loop of VC inverters

Therefore, one can augment the measured grid impedance model $Y_{L,m}$ into the above control block diagram to achieve a generalised plant structure as shown in Figure 2-5. The encapsulated part represents the closed loop model of the inverter which can be pursued as the plant for the VOI controller which is external to the generalised plant $P_{vc}(s)$. The external VOI controller can now be designed by applying linear robust control methods from literature such as mixed sensitivity H-infinity (H_∞) synthesis [15]. Note that a weighting matrix W_u is introduced to parametrise the controller.

By applying the VOI control, it can be shown that the impedance of the VC inverter reduces to (2). The virtually designed impedance is shown in blue. One can observe that the bandwidth of the outer voltage control (K_V) of the VC inverter is modified by the virtual term.

$$\boldsymbol{Z_{VC,voi}} = [\boldsymbol{I} + \boldsymbol{G_{dv}K_I}(\boldsymbol{I} + \boldsymbol{G_{di}K_I})^{-1}(\boldsymbol{K_v} - \boldsymbol{Y_{voi}})]^{-1}\boldsymbol{Z_{ol}} \tag{2}$$

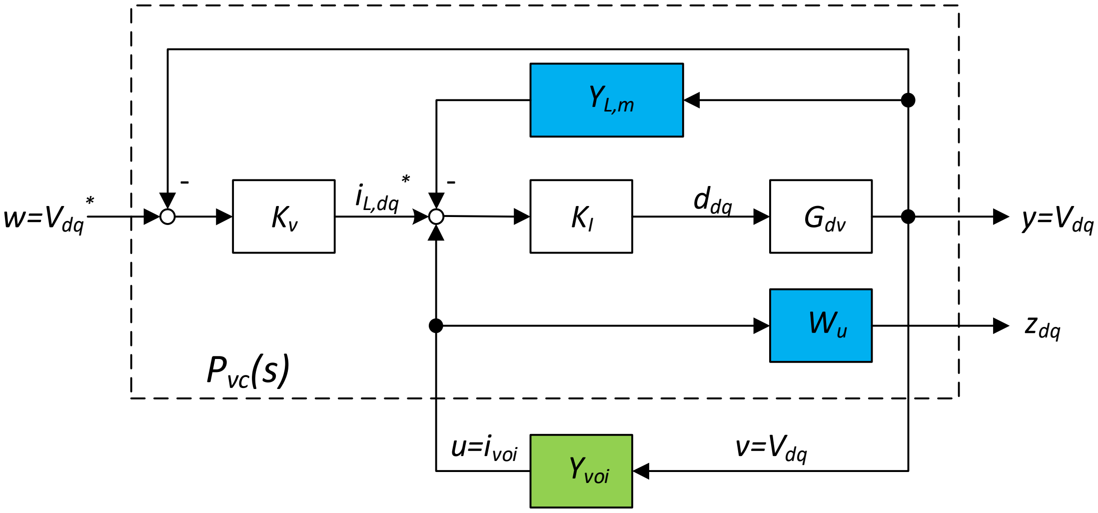

Figure 2-5 Generalised plant structure for VC inverter

2.2.2 VOI Design for current-controlled (CC) inverters

For CC inverters, the current set point comes from the power controller which in turn gets its set-points from the maximum power point tracker (MPPT) of the PV subsystem. The control block diagram of the CC inverter is shown in Figure 2-6. We follow a similar procedure as shown in the previous section to generate the generalized plant structure by augmenting the measured grid impedance model into control block diagram. The generalised plant structure of the CC inverter $P_{cc}(s)$ is shown in Figure 2-7. Similar procedures of VC inverters can be used for designing the VOI of CC inverters.

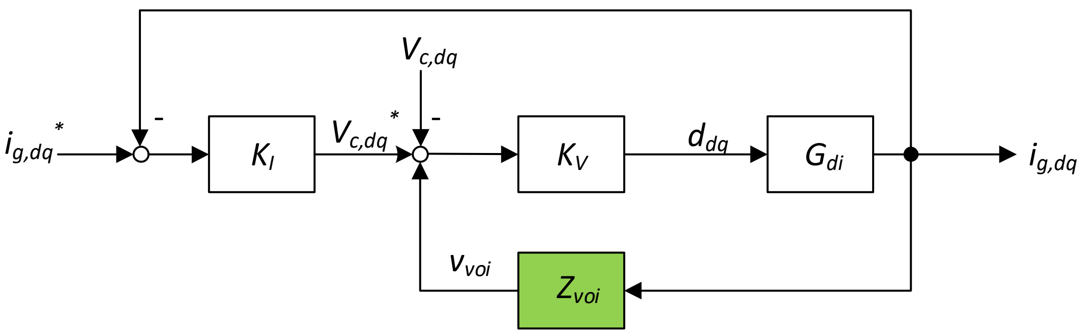

Figure 2-6 VOI loop of CC inverters

By applying the VOI control, it can be shown that the impedance of the CC inverter reduces to (3). The virtually designed impedance is shown in blue. One can observe that the bandwidth of the outer current control (K_I) of the CC inverter is modified by the virtual term.

$$\boldsymbol{Y}_{\boldsymbol{CC,voi}} = [\boldsymbol{I} + \boldsymbol{G}_{\boldsymbol{di}}\boldsymbol{K}_{\boldsymbol{v}}(\boldsymbol{I} + \boldsymbol{G}_{\boldsymbol{dv}}\boldsymbol{K}_{\boldsymbol{v}})^{-1}(\boldsymbol{K}_{\boldsymbol{i}} - \boldsymbol{Z}_{\boldsymbol{voi}})]^{-1}\boldsymbol{Y}_{\boldsymbol{ol}} \tag{3}$$

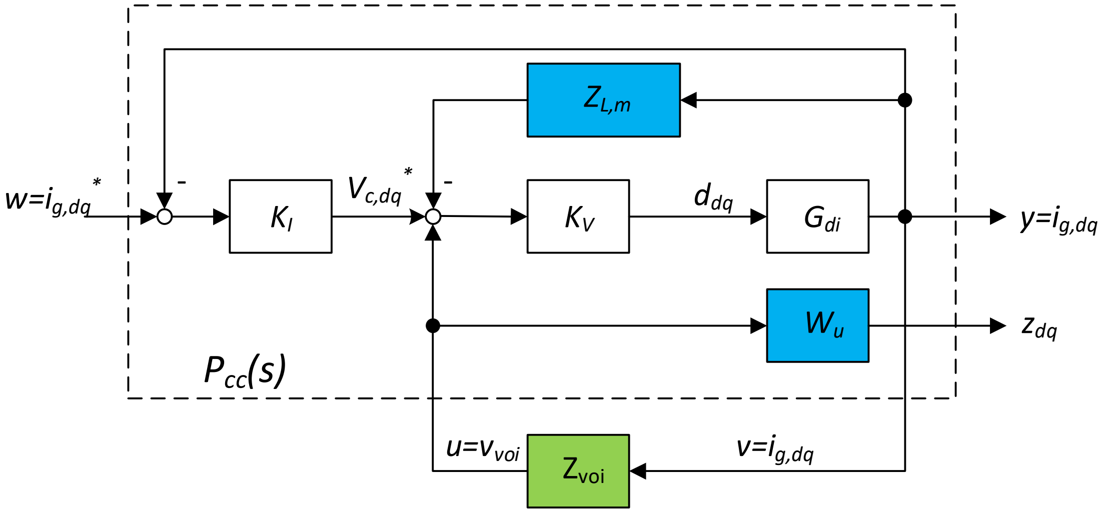

Figure 2-7 Generalised plant structure for CC inverter

2.2.3 System Level Implementation of VOI for DSO operators

As mentioned in earlier sections, after completion of the first two steps of the DVSM algorithm, the DSO operator has the impedance of the inverter and the impedance of the grid measured by the inverter. A software-based subsystem such as SERVO in ESB Networks can perform the calculations based on the linear robust control method to design the VOI control. Furthermore, since the VOI control design is parametrised based on the weighting function W_u, DSO operators can choose the appropriate weighting function such that dynamic stability margins are sufficient. With the proposed idea of a generalised VOI design for inverters, DSOs can actively control the dynamic operation of every inverter in the grid. More importantly, since the algorithms involved in SV_A are for automation, human influence can be minimised.

2.3 Results

2.3.1 Inverter VOI

The case of grid integrated power converter with a high order grid impedance is considered for the test scenario. Instead of a typical RL grid impedance, a higher order RLC impedance is chosen to incorporate harmonic resonance phenomenon of LVAC grids. As mentioned earlier, the VOI design is parametrised by the weighting function W_u which consists of gain parameter M_u and a bandwidth/cut-off parameter ω_u. The analysis of various VOI designed based on the parameter variation is discussed both in time and frequency domain.

A large signal load disturbance is injected into the system which causes to voltage waveform to have a sudden dip. The performances of the various designed VOI controllers are shown in Figure 2-8. All controllers are able to stabilise the grid and the best time domain performance corresponds to the case with M_u=3 and ω_u=30.

The frequency domain impedance of the VOI inverter as calculated from (2) is presented through the bode plots in Figure 2-9. In this case, the VOI was designed to significantly damp the harmonics around 1 kHz. The subtle variation of VOI with design parameters is more clearly visible upon zooming. It must be noted that the VOIs are designed for a fixed grid impedance model for showing the impact of design parameters. Notice that the overshoot, undershoot and settling times can be adjusted by modifying the impedance of inverters. We can influence the stability margins at the power electronic interface. Since the VOI control methods are based on robust stability theory, we can design controllers which guarantee robustness/passivity properties. This is explained in the next subsection with a stability analysis.

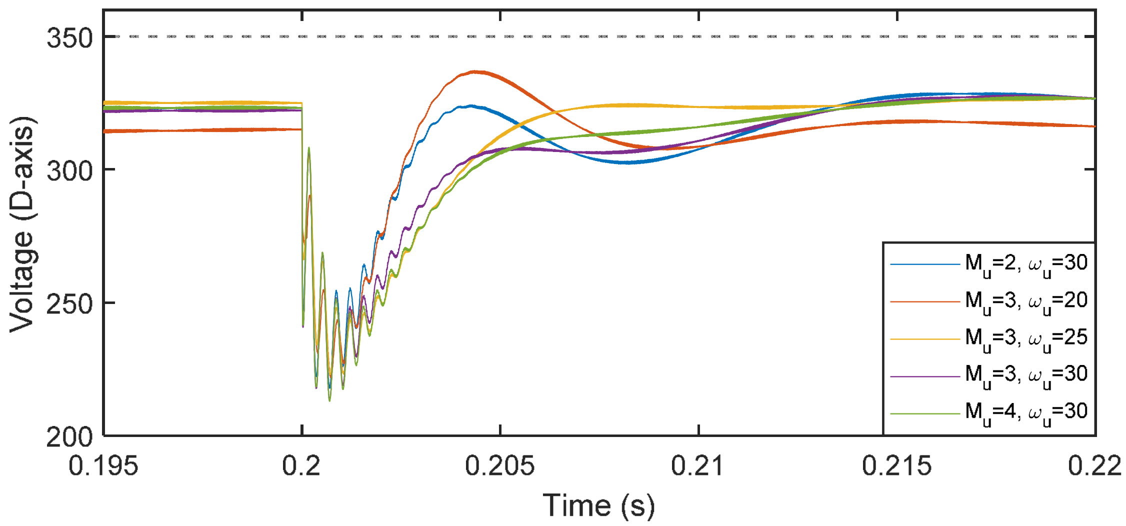

Figure 2-8 Time domain performance under large signal disturbance

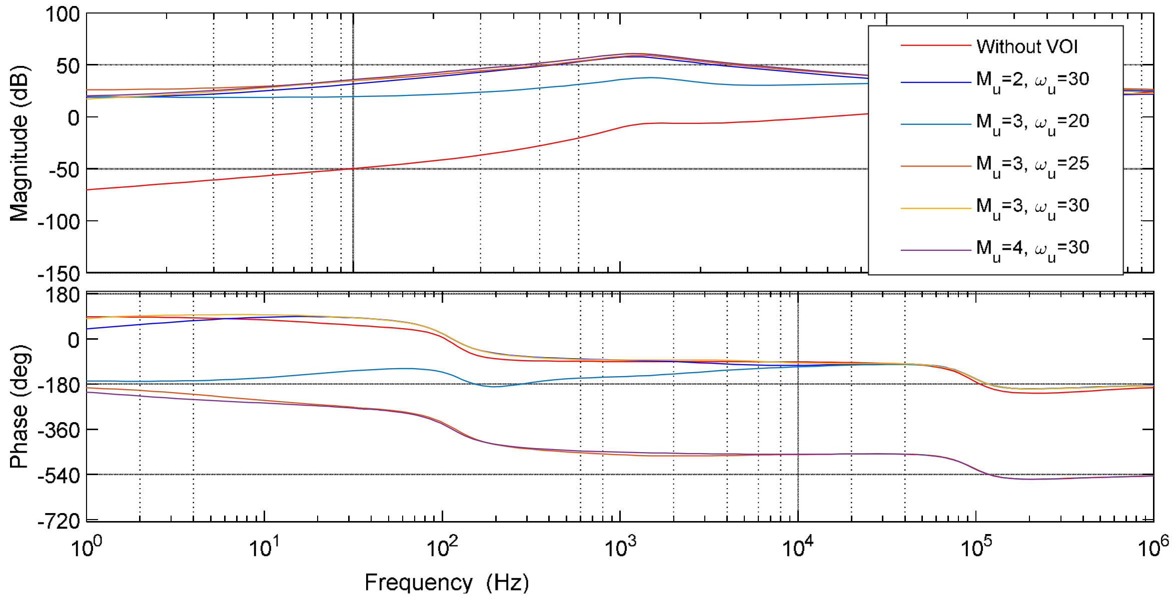

Figure 2-9 Inverter output impedance vs Frequency

2.3.2 Stability analysis of Inverter VOI

An impedance-based stability analysis is done based on GNC to analyse the impact of design parameters in the frequency domain. The method described in *D3.2* and *D3.3* is applied for the stability analysis. From Figure 2-10 and Figure 2-11, the two-design parameter combination can be compared and contrasted. Due to the conservative nature of characteristic loci of eigenvalue λ_1 in Figure 2-11 i.e. the locus exists within unit circle implying more stability. One can observe a stable time domain performance associated with this case compared to the case shown in Figure 2-10. Thus, the time domain simulation and frequency domain stability interpretation are coherent.

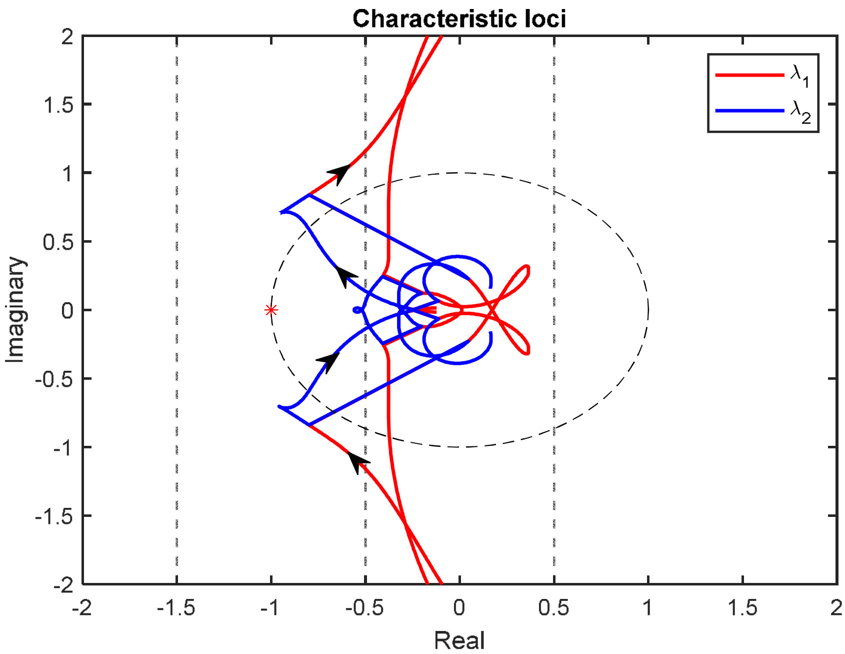

Figure 2-10 GNC based stability analysis: M_u=3 and w_u=30

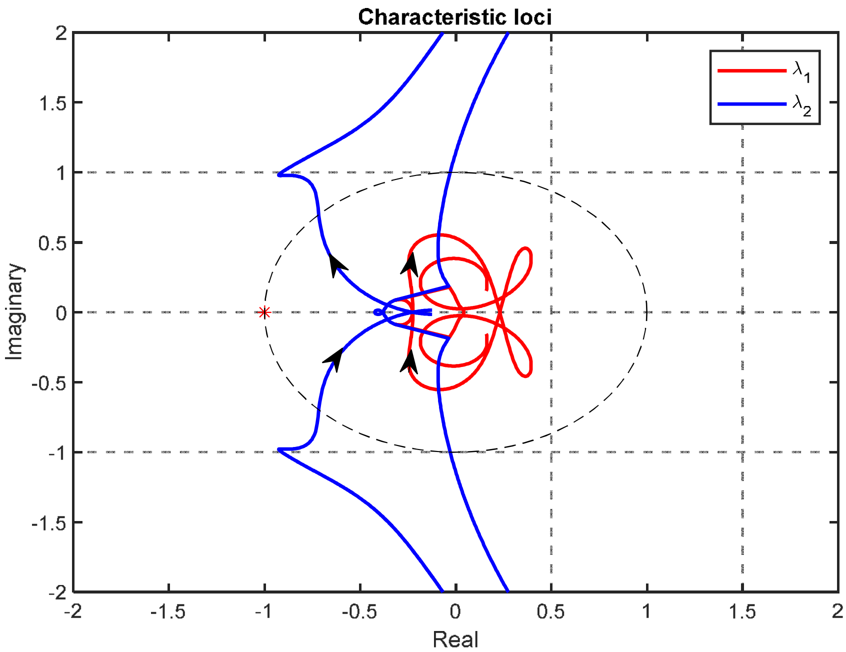

Figure 2-11 GNC based stability analysis: M_u=3 and w_u=20

2.3.3 Implications of new techniques on network codes

From the proposed technical work, we derive the implications of the new techniques on network codes. This will be later be used to draft ancillary services and network codes definitions.

2.3.3.1 New behavioural of RES inverters

In the context of decentralised control, the control command received from a tertiary level or from a Microgrid operator might be setpoints for real and reactive power in a conventional sense. However, the methods developed in WP3, envision a case where the higher level might modify the behavioural of the inverter. By behavioural we mean the control parameters themselves. The examples pertaining to WP3 are presented as follows:

- The Dynamic Voltage Stability Monitoring (DVSM) (SV_A) functionality which resides in the SSAU would send control commands back to the VOI controller, which will, in turn, modify the control parameters of the inverter to achieve the set-point impedance. Hence, the behavioural of inverters are modified here and since the SSAU sends these commands, the DSO grid codes must allow it.
- The Active Voltage Management (AVM) (SV_B) technique modifies the Volt-var Curves of the RES inverter. Hence the concept of Volt-var curve definition for house RES inverters must be included into the grid codes.

This deliverable addresses the new VOI behavioural requirements of RES inverters. Future work will show that the power factor of the inverter can be dynamically modified through VOI control which enables RES inverters provide advanced voltage support to the LVAC grid in a decentralised manner.

2.3.3.2 Decentralised Voltage Control

The proposed DVSM technique where every inverter in the grid actively takes part in the grid-support falls under the paradigm of decentralised control which paves the road towards high RES penetration in active LVAC grids. The inverter utilises the local knowledge through its WSI based measurement process and adapts its control loop for stable operation. A highly stable and passive grid is achieved when all the grid-tied inverters participate in local knowledge-based control. The stability monitoring process is governed centrally by the DSO operator in SSAU and 5G ICT infrastructure can used for communicating with the RES inverters as shown in Figure 2-1. We recommend the practice of decentralised control for LV distribution grids and we propose a grid code for decentralised voltage control which will allow DSO operators to actively monitor the grid-tied RES inverters.

Validation of DVSM algorithm will be undertaken in RWTH lab in Aachen using the HiL setup shown in Figure 2-12. The *HiL* setup consisting of OPAL-RT and Labview is already running and this setup is used to validate the WSI tool. An extension of this real-time simulation is the inclusion of the virtual machine (VM) where the stability monitoring algorithm and VOI calculations are implemented. This experiment will effectively demonstrate the idea of ICT driven decentralised control in futuristic distribution grids which DSOs can adopt.

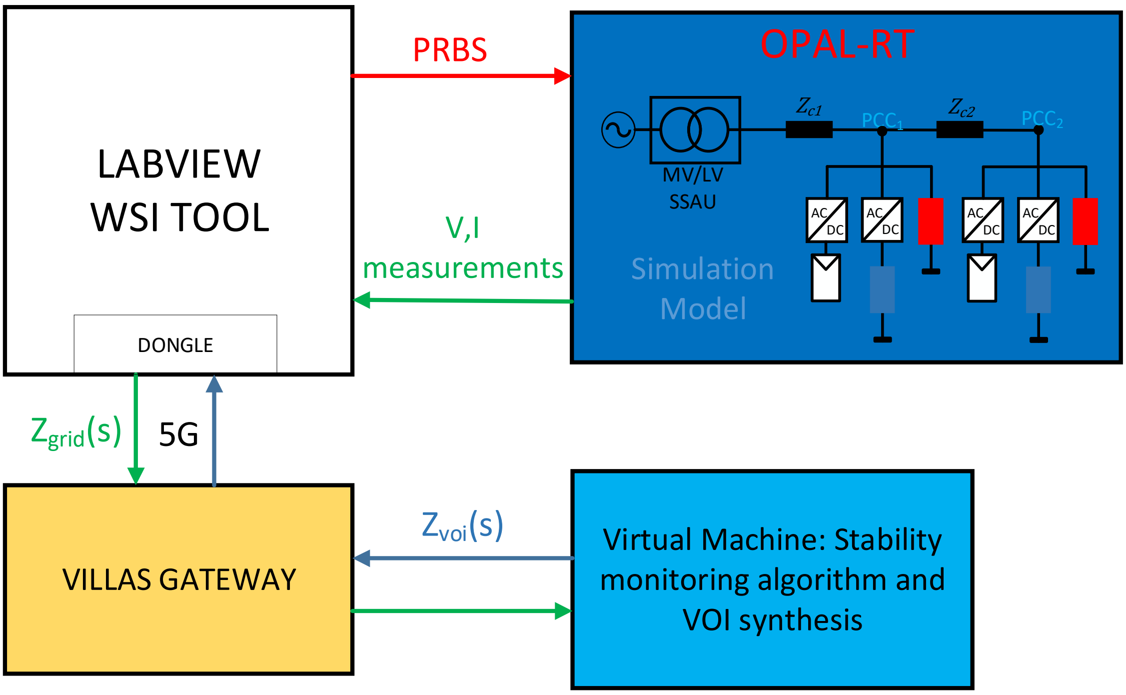

Figure 2-12 DVSM (SV_A) HiL Validation at RWTH lab, Aachen

2.3.3.3 Dynamic Stability Margins

With large number RES inverters in the LVAC grids, we envision a virtual impedance based decentralised control. For accessing the grid voltage stability, a stability monitoring algorithm is developed which is placed in the SSAU. The stability of such a dynamic system is assessed through dynamic stability margins such as gain and phase margins. In the current grid codes, there is no such a definition found. Hence for the futuristic grids, we propose the inclusion of dynamic stability margin definitions. Additionally, we envision through our work to determine minimum dynamic stability margin limits or thresholds that the system must possess.

Before performing the test in Ireland, a trial will be performed in RWTH lab in Aachen. The setup consists of a low power inverter connected to a passive load as shown in Figure 2-13. WSI which is local to the inverter measured the grid impedance, which is the known passive load in this case. The measured grid impedance data is communicated to a virtual machine (VM) which mimics the role of the SSAU. Stability monitoring calculations and VOI calculations are implemented in the VM.

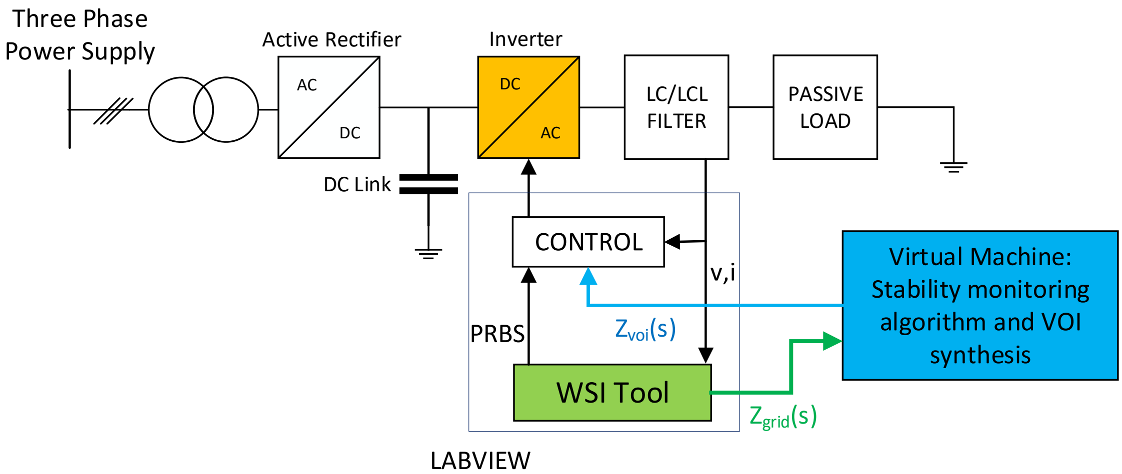

Figure 2-13 DVSM Field Trial in RWTH lab, Aachen

2.4 Conclusion

This chapter concludes the system-level monitoring concept definition for Dynamic Voltage Stability Monitoring SV_A scenario.

Review of various Virtual Output Impedance (VOI) and active damping techniques was performed. A gap was identified in the way VOI controllers were defined. Many of the methods do not take the time-varying nature of the grid impedance. Few of the methods that do consider grid impedance measurement do not have a generalised design procedure for the design of VOI controllers.

This deliverable addresses the above-mentioned gap by presenting a generalised framework for the synthesis of a class of robust VOI controllers based on the real-time grid impedance measurements. Parameters of the weighting function can be used to modify the inverter output impedance. Validation of the proposed technique is performed in both time and frequency domain in offline simulations.

The system-level implementation of the SV_A technique was analysed. Particularly, the placement of the WSI tool in the system. The first possibility is the inverter hosting the WSI tool locally. The controller hardware needs to be computationally powerful whereas the communication data volume is low. The second possibility is where the WSI tool is implemented centrally in SSAU. Here, the data volume is high although the controller of the inverter can be cheap.

The network code implications of the new technique are provided the and mapped simulation scenarios to validate and support the proposed network codes and ancillary services are presented.

3. System level monitoring concept based on Active Voltage Management technique (UCD)

3.1 Architecture of System Level Active Voltage Management

The effectiveness of the voltage control strategy widely depends on the accuracy of the system model which is used to extract such a strategy in the online applications. As decentralized approaches rely only on local measurements for system identification, the effectiveness of the control strategy may be compromised. On the other hand, centralize approaches suffer delay issues, low speed, communication errors due to contamination of measurement and command signals in communication channels, lack of enough measurements and some other issues.

The round-trip time of a complete cycle from the inverter to the point of calculation and back is important. The quicker the measurement and the required change can be communicated the more accurate and effective the control action. A longer delay between the instance of measuring the voltage level at PCC and the time of applying the new setting of reactive power injection for inverters of the controllable devices leads to less effective results. The delay includes both the measurement and the actuation delays that widely exist in real systems. For a centralized control system, this delay is higher which reduces the effectiveness of the control actions. In a decentralized control, this delay is lower. However, even a small reduction in this time delay can be a great help.

In this section, the structure of a hierarchical active voltage management algorithm is defined, where the decentralized (local) controllers try to solve the voltage problems and the higher level (system level) control keeps the local system identification results as accurate as possible. Under such a setup, the control strategies are quickly extracted by the local control systems to meet the real-time requirements of active voltage management in the current low voltage distribution systems and the system model applied in the local control systems is kept up-to-date by the system level control to mitigate the potential errors. Using the proposed method developed in **D3.4**, the parameters of the local AVM algorithm can be updated according to the network configuration and also the availability of the inverter-based controllable devices.

In **D3.2** and **D3.3**, the proposed local active voltage management algorithm was discussed. The focus was on the application of Volt-var Curves (VVCs) for determining the reactive power supports of the inverter-based controllable devices in an unbalanced low voltage distribution system. After application of VVCs and finding the new settings of each inverter, it is quite possible that more corrections are required according to the new set of PCC voltages. A supervised closed-loop control is proposed here to achieve a near optimal reactive power dispatch between the system controllable devices for better voltage control. Regarding this supervised control, the other task of the system level control is to initiate the control process to reach a balanced state.

This chapter also tackles another important subject. Considering the high penetration level of the RES in LV distribution systems, there may be some opportunities to control the load point voltages more effectively using these high control capacities. In this chapter, a framework is developed to consider different objectives at the same time in the proposed method for AVM. This leads to the exploitation of the system control capacity. The voltage control objective(s) should be determined by the system level control according to the system needs and control capacity.

3.1.1 Local Measurements Requirements for System Level Voltage Management

The data requirements for local (decentralized) control were discussed in **D3.4**. Here we summarize these data in the following list, then the data requirements for system level control will be explained.

The Data required for decentralized AVM algorithm is described as follows:

- Network configuration (the three phase diagram)
- Line characteristics
- Fixed reactive power compensators
- The historical load levels and load model parameters (ZIP coefficients) at each load point.
- Maximum capacity of the inverters
- Inverter type, connection type (star or delta).

- Historical data on the energy generation of RESs.
- Inverter mode of operation (Power control mode or voltage control mode)
- Operator Objectives such as minimisation of voltage deviation from a desirable value, minimisation of voltage unbalance, minimisation of active power losses and so on.
- Inverter impedance as a function of frequency (viewed at the connection point of each inverter).
- Voltage at inverter connection point
- Active and reactive power injection of the inverters before developing the voltage control strategy.
- Additional limitations of the inverters, such as maximum power angle (regarding minimum permissible power factor).
- Network impedance viewed by the inverter from the connection point.

In this chapter, a supervised decentralized control approach will be discussed. In the unsupervised decentralized approach presented in **D3.2**, **D3.3** and **D3.4**, first the voltages are measured at PCCs. Based on these voltages and using VCCs, the value of the change in the reactive power support of all inverters will be determined. However, for two reasons the final voltage set at PCCs may not match the optimal voltages or target voltage set. The first reason is that the operational constraints of the inverters for each type of control devices (see **D3.3**) may restrict the voltage control capability of the set of inverter-based controllable devices installed across the network. The second reason is that the VVCs are obtained using a linear regression technique which gives an approximately optimal reactive power setting. There would be some unpredicted states for which the final voltages (after applying the new control settings) would never match the target voltages.

A supervised control is able to solve the problem while keeping the decentralized structure of the decentralized control system. This supervised control framework benefits the advantages of both centralized and decentralized control systems. In this sub-section, the data that should be passed from the local control system to the central control unit and vice versa will be discussed. The next sub-section discusses this supervised closed-loop AVM algorithm.

The data which should be communicated from the central control unit to each local control system are listed below:

- Network configuration
- Availability of the system controllable devices
- The objectives that the local control should seek
- Control commands (when a balanced state has not yet been reached)

Regarding the objectives that may be considered by the DSO, a discussion will be provided later in this chapter. The main important change concerning **D3.3**, is that in this section, the basic foundations of the multi-objective active voltage management algorithm is developed to better exploit the control capacity available in the system. In this way, the operator's objectives are better satisfied in improving the service quality.

It should be noted that according to the framework provided in **D3.4**, the local control system of each RES is able to approximate the network configuration and also deduce the availability of the controllable devices by tracking the system impedance viewed from the regarding PCC. This fast local system identification approach enables the local control system to make the decision based on the last updated characteristics of the system. However, in the case that the data provided by the local system identification unit is not accurate enough, the network configuration and also the availability of the system controllable devices will be communicated from the central control unit to the local control systems.

The data which should be communicated from each local control system to the central control unit are listed below:

- Target voltage
- Upper and lower bounds on the reactive power support that can be provide by this controllable device (according to operational constraints of the regarding converter)
- Last measured voltage at PCC
- Current reactive power injection at PCC

3.2 System Level Monitoring and Decentralized Active Voltage Management

In the future low voltage grids, with multiple inverter-based sources connected, voltage regulation may become a critical task. The potential exists for inverter interfaced sources to be deployed to regulate the voltage at the point of common coupling (PCC) of each inverter-based controllable device. The PCC voltage regulation is attainable with inverter interfaced sources by dynamically controlling the amount of reactive power injected into the power distribution grid by individual systems.

In **D3.2, D3.3,** and **D3.4** a framework was developed for local voltage management based on the local measurements and Volt-var curves. This framework proposed a static voltage control in which the reactive power injections of the controllable devices were found to achieve a certain objective. The performance of the proposed decentralized voltage control in improving the operator objectives was proven in D3.3. However, after applying this framework it is quite possible that further corrections are required since a balanced state may not be reached. In this section, a closed-loop control is proposed to deal with this issue. This control structure dynamically controls the voltage at PCC of the system inverter based controllable devices.

3.2.1 System Level Voltage Management

In **D3.4**, the plant models of the PCC voltage controller of the inverter-based devices were derived considering both reactance and resistance of the network to which these devices are connected. Different inverter-based controllable devices, i.e., PV, V2G, battery and any other types of controllable systems were evaluated to identify a suitable compensator for the open-loop PCC voltage controller to regulate the PCC voltage at a given reference voltage in the voltage control mode of operation or to find the reactive power compensator of the controllable devices. Simulation studies in **D3.2**, **D3.3**, **D3.4** and experimental verification reported in **D5.2** confirm that the theoretical approach taken to derive the control plant model of the PCC voltage controller is effective and the procedure that is followed to design the controller is robust. The control design procedures illustrated in the current research leads to a PCC voltage control system with acceptable dynamic and steady-state performance.

In this chapter, first, a supervised closed-loop controller is proposed to regulate the PCC voltage of the inverter-based RES systems that is connected to a single-phase or three-phase power distribution feeder (with a relatively high R to X ratio for the impedance seen from the PCC of each controllable inverter). Then, a multi-objective framework is considered to optimally exploit all the control capacity of these highly controllable devices according to the needs dictated by the system level control.

Based on the simulations conducted in **D3.2** to **D3.4**, the proposed voltage control technique based on VVCs is able to improve the system operation and to better satisfy the DSO's objectives. However, after application of VCCs to find the new reactive power injections of the controllable devices, it is quite possible that we do not achieve the optimal voltages. In order to elaborate on the sides of the issue, it should be noted that though by applying the VVCs for optimisation of the reactive power dispatch, the performance metrics will be improved (compared to the fixed power factor assumption and uncontrolled dispatch), the results are not globally optimal. Actually, the globally optimal results cannot be achieved using any decentralized control system. Therefore, the results of the proposed AVM algorithm can be further improved by a new round of applying the VVCs for obtaining the new reactive power setting for the system controllable devices, based on the new voltages achieved after applying the results of the previous round of voltage control based the proposed local AVM algorithm. In other words, after first round of applying the VVCs to find the optimal reactive power injection of all inverters, the set of voltage measurements will be updated. It is quite possible that according to these new voltage levels, further corrections are required.

Each inverter can start a new round of voltage control based on the available voltage measurement and the regarding VVC. However, it is possible that without a proper supervision, such actions lead to the fluctuation of the reactive power settings of the system controllable devices. In case of weak networks, this may even lead to an uncontrolled situation which would never converge to a stable situation. This indicates the need of applying a supervised closed loop voltage control based on the prosed local active voltage management using the VVCs extracted in the offline **system level** studies.

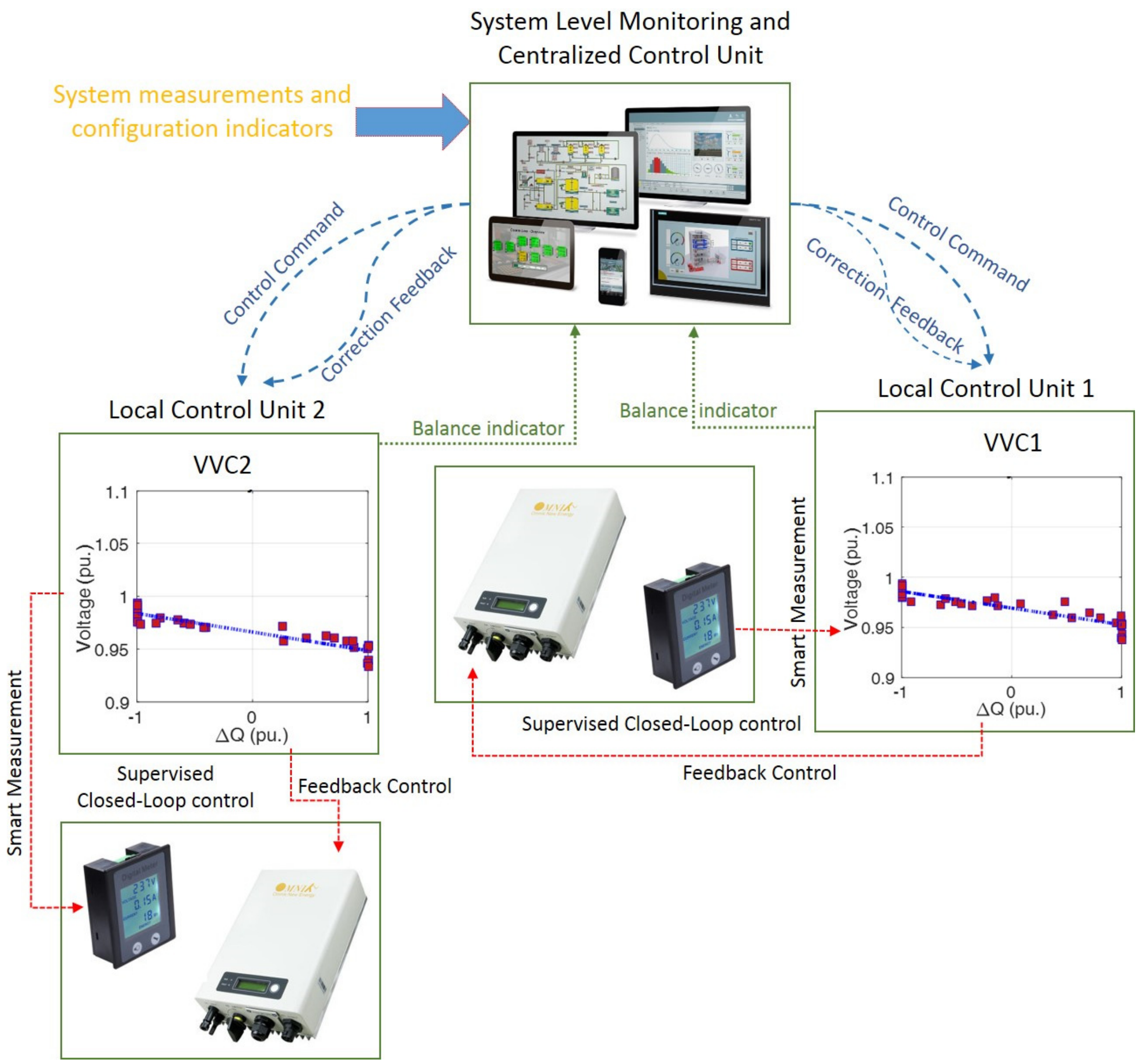

Figure 3-1 Proposed structure for supervised AVM algorithm

The balance points of each VCC are, $Q=Q^{max}$, $Q=Q^{min}$ and of course $V=c$ which is approximately equal to the target voltage of the regarding inverter. This indicates that after a successful application of the VVCs for the active voltage management in a low voltage distribution system, the reactive power or voltage settings at the PCC of **all** inverter-based controllable devices should be set at one of these balance points, signifying the fact that the required reactive power support is optimally dispatched between the system controllable devices to achieve a predefined system level objective or there is no other way to further optimise these settings due to the practical limitations on the reactive power supports that can be provided by each inverter, e.g., capacity limit. More discussions regarding these practical limitations that depend on the type of controllable devices under study can be found in **D3.3** and also **D3.8**.

Based on this discussion, the remaining part of this subsection is dedicated to provide a summary of the proposed supervised closed-loop decentralized active voltage management algorithm. Figure 3-1 presents a schematic diagram of the proposed supervised AVM algorithm.

- **Local control system**

  1) System identification:

  1-1) Identify the network topology and controllers' availability according to the impedance measured at the PCC of the regarding inverter periodically (see **D3.4**).

  1-2) Keep the identified model up-to-date.

1-3) Verify the identified model according to the data received from the system level central control unit.

2) Real-time control:

2-1) Wait for the control command from central control unit or initiate a new periodical round of voltage control

2-2) Measure the voltage at PCC when a new control command is received or at the instance of the periodical control routine.

2-3) Use the proper VCC according to the system characteristics identified in steps 1-3 and also the objective that is dictated by the central control unit to be followed. As discussed in D3.3, if some of the inverters are working under voltage control mode of operation, they should be tasked with following their target voltages (which also depend on the network configuration, availability of the other inverters and more importantly the system level objective for active voltage management).

2-4) Communicate the balance state to the central control unit. In this stage, the reactive power injection, new voltage level, minimum and maximum allowable reactive power injection and target voltage is communicated.

- **Central control unit**

1) System level analysis

1-1) Identify the network configuration and availability of the controllable devices.

1-2) Decide on the system level objective to be followed by the local control systems.

2) Real-time control

2-1) Analyse the data received from the local control systems.

2-2) Initiate the new control command if a balanced point has not been reached yet.

2-3) Stop sending the control commands if the control settings of the controllable devices are not significantly changed for two consecutive control rounds or the average distance of the PCC voltages from the target voltages is increasing (to avoid fluctuation of the PCC voltages around the target voltages).

3.2.2 System Level Objectives in the proposed supervised Decentralized AVM Algorithm

In the active voltage management of low voltage distribution systems, the main objective depends on the system needs and also the availability of the controllable devices that can effectively satisfy such objectives. In these systems, the availability of DERs and other controllable inverter-interfaced devices, enable the system operator to control the load point voltages more effectively to achieve a variety of objectives. In this project, three main objectives are considered for the active voltage management in futuristic low voltage distribution systems. These objectives are presented in Table 3-1.

Table 3-1 Objective menu

Code	Objective
1	Voltage unbalance improvement
2	Loss reduction
3	Improvement of voltage deviation ($V_{desired}$=1 pu.)

4 Multi-objective AVM

This section extends the existing AVM methodology presented in **D3.2**. The objectives of the active voltage management depend on the system needs and also the availability of the controllable devices that can effectively satisfy such objectives. In a low voltage distribution network with high penetration of RES and other controllable inverter-interfaced devices, there may be some opportunities to control the load point voltages more effectively using these high control capacity. Here, it has been tried to develop a framework to consider different objectives at the same time in the proposed method for active voltage management. Sometimes these objectives are incomparable and even opposing. Thus, the application of an efficient multi-criteria decision-making technique is proposed. A multi-objective active voltage management is developed to extend the works accomplished in **D3.2**. The proposed multi-objective framework considers needs and priorities of the distribution system operator’s and satisfies these objectives simultaneously.

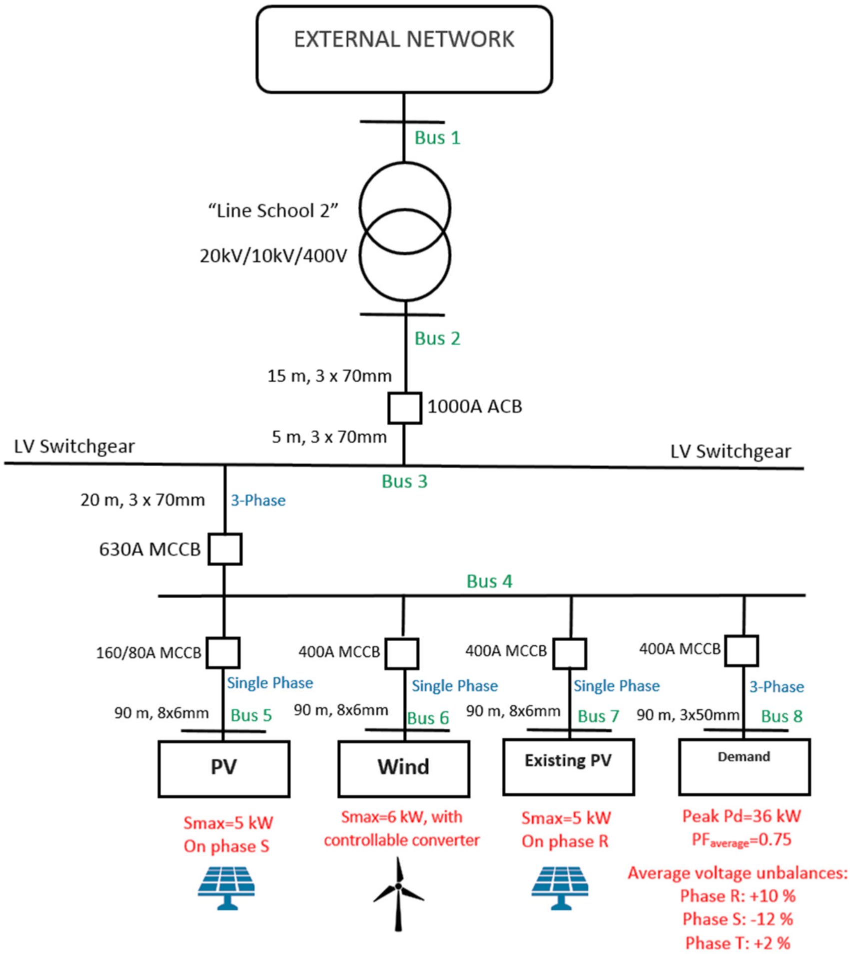

Figure 3-2 Simple low voltage distribution system for analysing the effects of various objectives on each other

A very simple example is considered here to explain how the available reactive power support capacity in low voltage networks can be exploited to satisfy more than only one objective. This simple low voltage distribution system is presented in **Figure 3-2**. This is a simplified system based on a real system in Portlaoise, Ireland. Useful data are also presented in this figure. Let’s focus on the single scenario to be able to present the voltage profiles in different studies. **Table 3-2** presents the active and reactive demands on different phases, ZIP load characteristics (see deliverable **D3.2**, **Section 3.2**), active power production of each PV and active production of wind turbine, in this scenario.

Table 3-2 Single scenario data for the simple example presented in Figure 3-2

Active power demand at bus 8 (kW), phase R/T/S	9.55/7.22/8.65
Reactive power demand at bus 8 (kVAR), phase R/T/S	4.63/3.50/4.19
Load factor at bus 8	70%
Load Z coefficient at bus 8	0.4
Load I coefficient at bus 8	0.2
Load P coefficient at bus 8	0.4
Active power production of new PV (kW)	0
Active power production of existing PV (kW)	0
Active power production of wind turbine (kW)	0

In this simple example, the optimal voltages have been obtained considering the voltage unbalance minimisation as the only objective. In order to analyse the effectiveness of the proposed method for optimising the voltage unbalance in the first scenario (Table 3-2), the voltages of all three phases have been depicted in **Figure 3-3**. These voltages are also depicted in **Figure 3-4** considering, with the fixed power factor criterion for the operation of all inverters of the available RESs. As can be seen, the proposed algorithm has effectively reduced the voltage unbalance at the load point, i.e., bus 8 of this small low voltage distribution system. The optimal value of voltage unbalance in this scenario is 0. The value of voltage unbalance for common industry practice, i.e., Power Factor (*PF*)=0.95 is 0.35%.

However, as can be seen, as a result of applying the optimal set-points (reactive power injected by the system inverters) found considering voltage unbalance minimisation as the objective of the active voltage management algorithm, the average voltage deviation of three phases has increased, i.e., the voltages at load point are more deviated from 1 pu., which is not desirable. Quantitative results show that, with this objective, the voltage deviation is 2.4 for optimal control plan. For the fixed power factor strategy (*PF*=0.95), the value of total voltage deviation is 2.2%. The load level is not very high in this scenario. With higher load levels, this problem is more severe due to higher values of the voltage drop across the network lines.

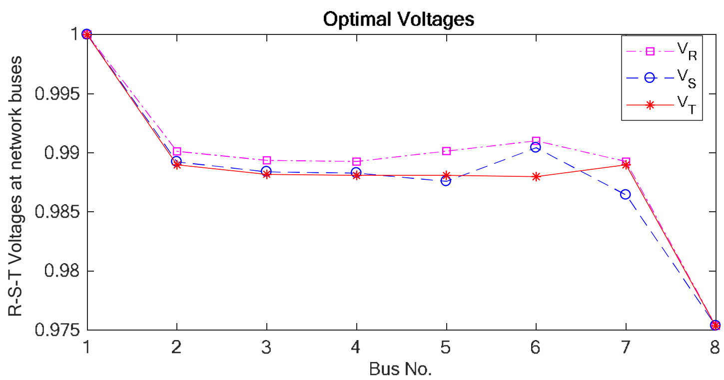

Figure 3-3 Optimal voltage levels at system buses, single-objective (minimisation of voltage unbalance).

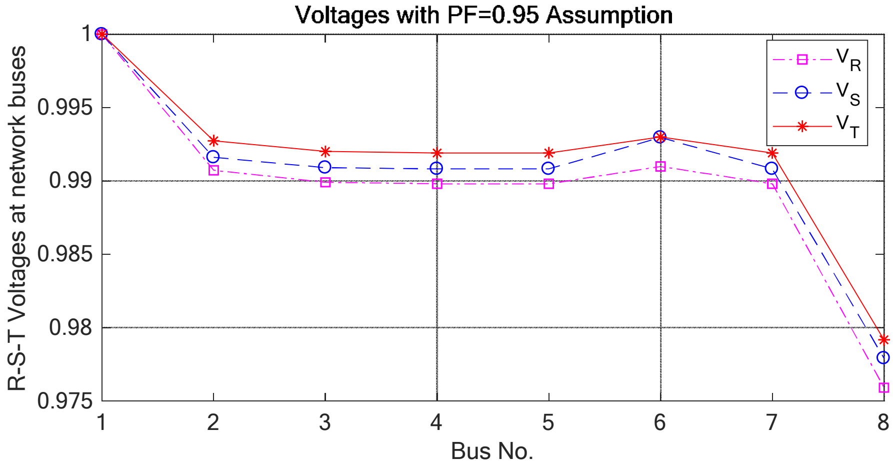

Figure 3-4 Voltage levels at system buses, fixed power factor criterion for reactive power support (PF=0.95).

In a separate study, the objective is changed to minimisation of the voltage deviations from 1 pu. **Figure 3-5** shows the voltage profiles for each phase at the load point (bus 8 in Figure 3-2). Comparing this figure to the voltage levels presented in Figure 3-3 and Figure 3-4, it is obvious that the voltage deviation has been improved. The value of voltage deviation is 1.4% in this study. However, with the optimal reactive power control plan extracted in this study, the voltage unbalance is about 0.38% which is even higher than the voltage unbalance associated to the fixed power factor strategy (*PF*=0.95).

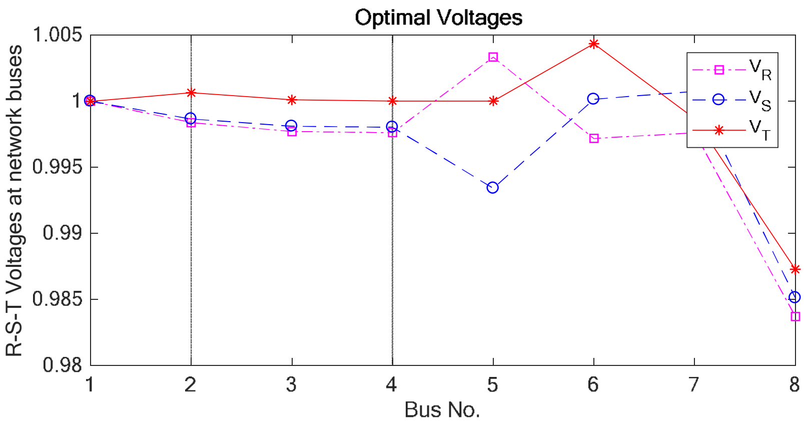

Figure 3-5 Optimal voltage levels at system buses, single-objective (minimisation of average voltage deviation).

Looking at the results obtained for this simple example, one can say that with this high control capacity (three controllable RESs), there may be some opportunities to control the load point voltages more effectively. Here, it has been tried to develop a framework to consider both objectives at the same time in the proposed method for active voltage management. Looking at these objectives, it is obvious that they are incomparable and may be opposing. This indicates the fact that the regarding objective functions cannot be summed up to give a single objective function. Therefore, the application of an effective multi-criteria decision making (MCDM) method is inevitable. This method should be able to compare the values of these objective functions for a proposed decision.

Here, fuzzy multi-objective decision making (FMODM) method is applied [16]-[17]. This method is briefly introduced here. A more detailed discussion is provided in Appendix A. FMODM belongs to a wide category of the MCDM approaches which are called outranking methods. In contrast to the other methods, the outranking methods have the characteristic of allowing incomparability between alternatives. This characteristic is important in situations where some alternatives cannot be compared for one or another reason.

As explained in Appendix A.1, in the fuzzy domain, the degree of satisfaction of each objective is specified by a value between 0 and 1 (signifying the worst and best possible objective function values). In this method, firstly, the best and worst values of each objective function should be found. A single-objective optimisation was conducted to find the optimal set-points of the network inverters to find the best value of each objective function. In order to find the worst value of this objective function, the value of this objective function is calculated without applying any reactive power support.

According to the proposed multi-objective framework and the single objective studies on this simple low voltage distribution system, the best and worst values of the first objective function (voltage unbalance) is 0 and 0.35%, respectively. The best and worst values of the second objective function are also 1.4 and 2.2%, respectively. The membership functions of the first and second objectives are presented in **Figure 3-6**. As can be seen, the degree of satisfaction of the first and second objectives increases monotonically as the value of each objective function decreases from Obj^{max} to Obj^{min}.

For each solution vector (including the value of the reactive power injection of all inverters). The values of these objective functions, i.e., voltage unbalance and voltage deviation objective functions, are calculated according to the explanations provided in deliverable **D3.2**. The values of membership functions of voltage unbalance and voltage deviation problems ($\mu_1(X)$ and $\mu_2(X)$) are found next using the membership function provided in **Figure 3-6**.

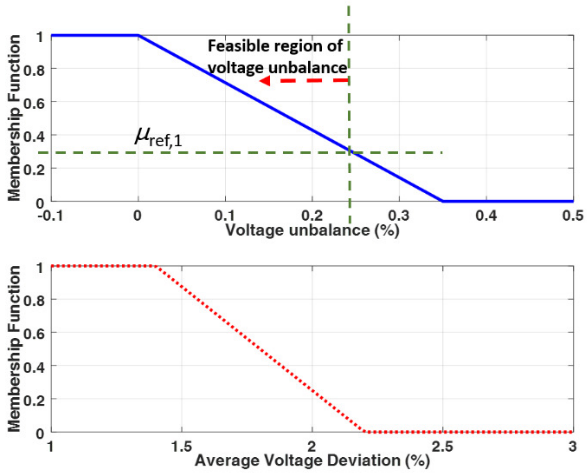

Figure 3-6 Membership functions of the problem objectives (minimisation of voltage unbalance and minimisation of average voltage deviation).

The final fitness function is provided in **(3.1)**. The optimisation tries to maximize this fitness function.

$$\max_X \{\mu_1(X)+\mu_2(X)-p_1(X)-p_2(X)\} \quad \textbf{(3.1)}$$

$$p_i(X)=\begin{cases} W.(\mu_{\mathrm{ref},i}(X)-\mu_i(X)) & \mu_{\mathrm{ref},i}(X)>\mu_i(X) \\ 0 & \text{otherwise} \end{cases} \quad \textbf{(3.2)}$$

To define a more controllable significance level for these objectives, after extracting these membership functions, the decision-maker is asked to specify the minimum achievement degree of each membership function, i.e., reference membership function μ_{ref}, which takes the real values between 0 and 1. Higher values of this parameter show more importance, and hence give more weight to the regarding objective. In this system, in order to give the same importance level to both objectives (minimisation of voltage unbalance and minimisation of average voltage deviation), μ_{ref} is assumed to be 0.4 for both objectives. The value of reference membership function introduces a constraint on the value of each objective function as depicted in **Figure 3-6** for the first objective (minimisation of voltage unbalance). The optimisation algorithm tries to satisfy these minimum allowable membership function constraints as the soft optimisation constraints by forming a penalty function, i.e., p_i in equation **(3.2)**, for each constraint (according to Appendix A) and appending this constraint to the objective function using a big *M* constant (Appendix A). The value of both *M* constants is assumed to be 100 signifying a constraint violation tolerant of 0.02 (see Appendix A).

Using this membership functions and applying the multi-objective fuzzy optimisation technique, a solution is achieved that satisfies both objectives as much as possible. The three-phase voltage levels at all network buses are depicted in **Figure 3-7**. As can be seen, both voltage unbalance and voltage deviation have been improved simultaneously compared to the results presented in **Figure 3-4** for the system with fixed power factor strategy (PF=0.95) for reactive power support. The values of these objective functions are 0.22% and 1.67%, respectively.

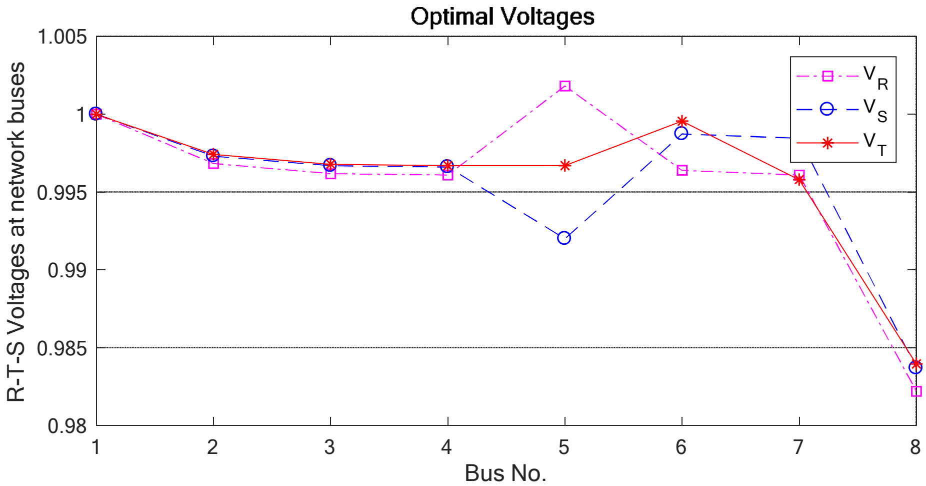

Figure 3-7 Optimal voltage levels at system buses, multi-objective (simultaneous minimisation of voltage unbalance and average voltage deviation).

3.3 Simulation Results

In this section, the results of applying the proposed AVM technique are first compared with those obtained by centralized control and also fixed power factor operation strategy as the industry common practice.

The effects of considering multi-objective framework are also analysed based on the results obtained via different studies on the same real case low voltage distribution system like the one used in **D3.2**. The proposed active voltage management technique is applied to find the Volt-var-curves with different objectives and the results are compared with the VVCs obtained using the multi-objective framework.

The sample low voltage distribution system which is used in this chapter to showcase the system level AVM technique is a radial LV feeder with 85 nodes situated in Ireland [18]–[21]. The data required for conducting the simulations can be found in **D3.3**.

The RESs available in the studies of this chapter are inverter-based 2 kW Vehicle to Grid (V2G) systems. The data on these V2G inverters are available in **D3.3**. We have made all the same assumptions as those presented in **D3.3** to make the results of these studies comparable to those obtained in that deliverable.

3.3.1 Results of Applying the Proposed Supervised Closed-Loop Control

The low voltage distribution system which is used here to showcase the supervised closed-loop AVM technique, and extract the VVCs for a set of inverter-based controllable devices in a multi-objective framework, is a radial LV feeder with 85 nodes situated in Ireland which was also used in **D3.3**. The required input data can be found [18]–[21]. Similar to **D3.3**, in this chapter, it is assumed that at the head of the feeder in the multi-scenario case, a separate feeder connection off the transformer supplies further 85 customers. This system was fully introduced in **D3.3**. In this chapter, it is assumed that the controllable devices are 9 V2G systems installed at different locations across this network. The batteries of Electric Vehicles (EVs) have a considerable potential not only to provide energy for the locomotion of EVs, but also to dynamically interact with the low voltage electricity grids.

Similar to **D3.3**, it has been assumed that these inverters have the bidirectional reactive power exchange capability, but the active power can only be absorbed by these inverters. Some computer simulations were conducted in **D3.3** and the VVCs were obtained for this test system.

Figure 3-8 (a) and (b) show the target voltages for minimisation of the voltage unbalance and loss minimisation, respectively. For the sake of brevity, only the target voltages are depicted. The slopes of the VVCs can be found in **D3.3** for both objectives. As can be seen, the target voltages are higher considering minimisation of the voltage unbalances as the objective comparing to the target voltages found for loss minimisation. The reason lies under the fact that with the lower voltages the active and reactive demands are lower at different load points due to the voltage-dependent nature of the system loads. These lower demands cause lower line currents which in turn lead to lower power loss.

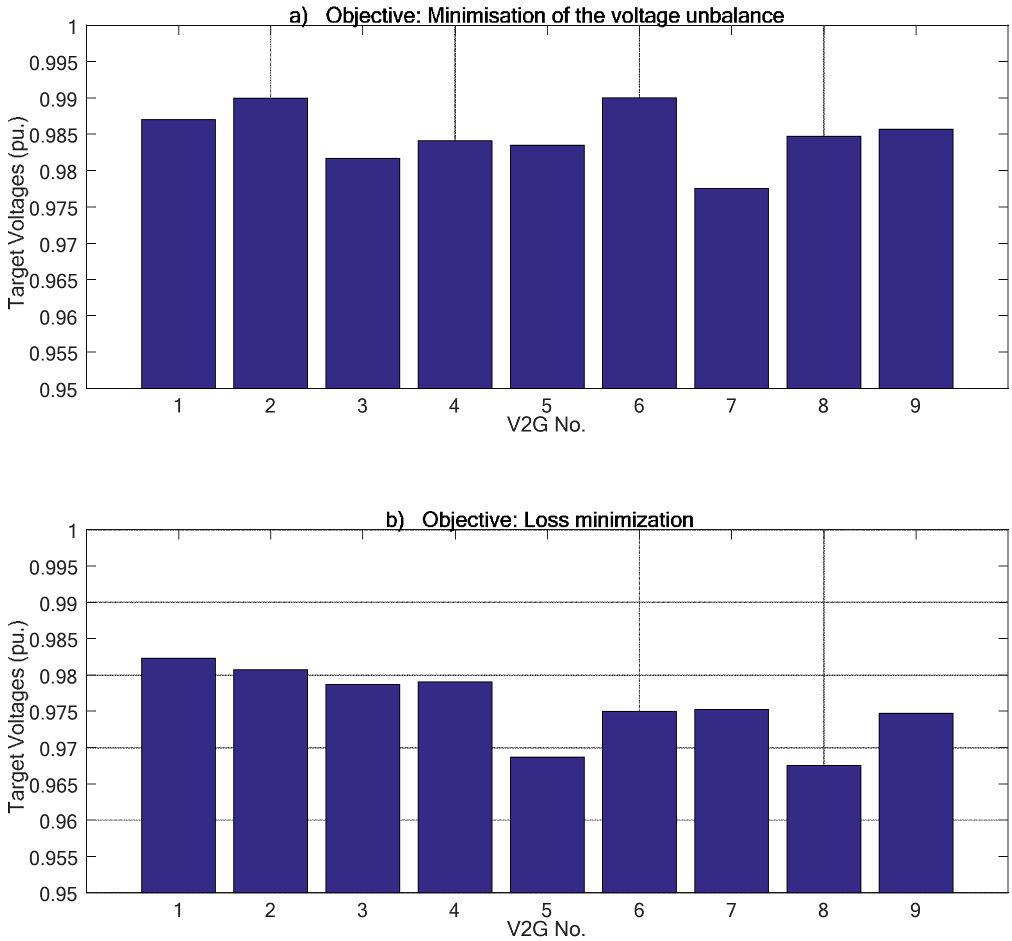

Figure 3-8 target voltages with minimisation of the voltage unbalance (a) and loss minimisation (b) as the system level objectives

In this sub-section, the performance of the proposed supervised AVM algorithm is analysed. As proposed in subsection 3.2.1, the central control system sends control commands and receives the balance status of the local control systems. This central control unit stops sending the control commands if the control settings of the controllable devices are not significantly changed for two consecutive control rounds or the average distance of the PCC voltages from the target voltages begin to increase. This helps to avoid fluctuation of the PCC voltages around the target voltages. Here, this control structure is applied and the average voltage deviation (AVD) from the target voltages is monitored to analyse the efficiency of the proposed voltage control algorithm. Further information regarding this algorithm can be found in subsection 3.2.1.

To calculate the value of AVD after each round of control, a three-phase power flow is first conducted to find the voltage at PCC of each inverter *i* (V_i) after applying the reactive power setting, proposed by the VVC of this inverter. The distance between the target voltage and the new voltage level of this inverter (V_i^{opt}-V_i) is then calculated. The mean square error of the voltages at all PCCs is considered as AVD. This index is monitored in two studies (for minimisation of the voltages unbalance and loss minimisation as the system objectives) until one of the stopping criteria is met.

For the most probable operation scenario in the operation of the sample system of this subsection (see D3.3), the proposed centralized closed-loop local active voltage management is applied to find the optimal setting of the V2G systems. The actual operational constraints are considered to limit the reactive power support that can be provided by each V2G system (see **D3.3**). The AVD is depicted in **Figure 3-9** and **Figure 3-10** for consecutive rounds of control for minimisation of the voltage unbalance and loss minimisation, respectively. For the first study, the central control system stops sending the control command after 5 rounds of control since after the fifth round of applying VVCs the begins to increase. After applying the final reactive power control strategy's, the voltage of no inverter matches the regarding target voltage and 4 inverters are supplying the maximum allowable reactive power due to their regarding operational limitations. In the second study, the central control unit stops sending control commands after 4 iteration since all the inverters reach a balanced condition (see subsection 3.2.1), i.e., one of the PCC voltages reaches the regarding target voltage, 4 inverters cannot provide any power support due to operational constraints and their active power consumption levels and other inverters are absorbing the maximum reactive power possible (due to their operational constraints) to reduce the value of the AVD. As can be seen, the value of AVD indexed is improved for both cases, signifying the efficiency of the proposed supervised closed-loop AVM algorithm.

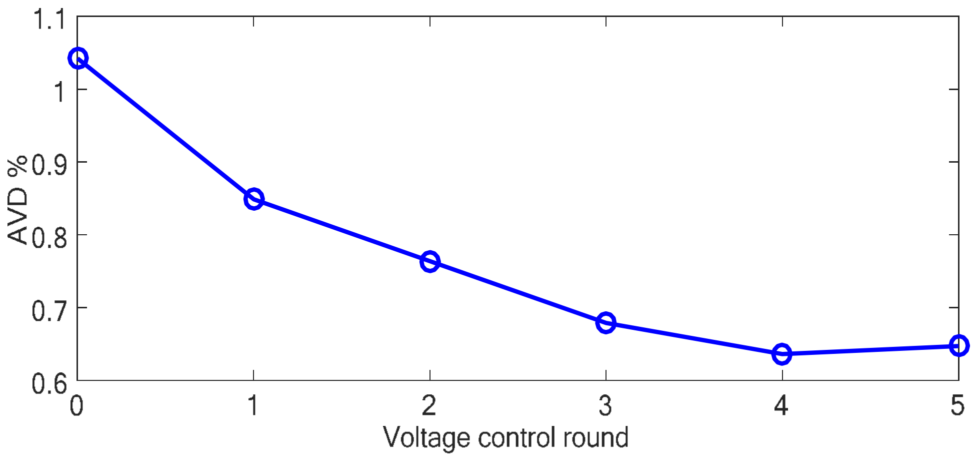

Figure 3-9 Average voltage deviation from the target voltages in consecutive rounds of control, objective: minimisation of the voltage unbalance.

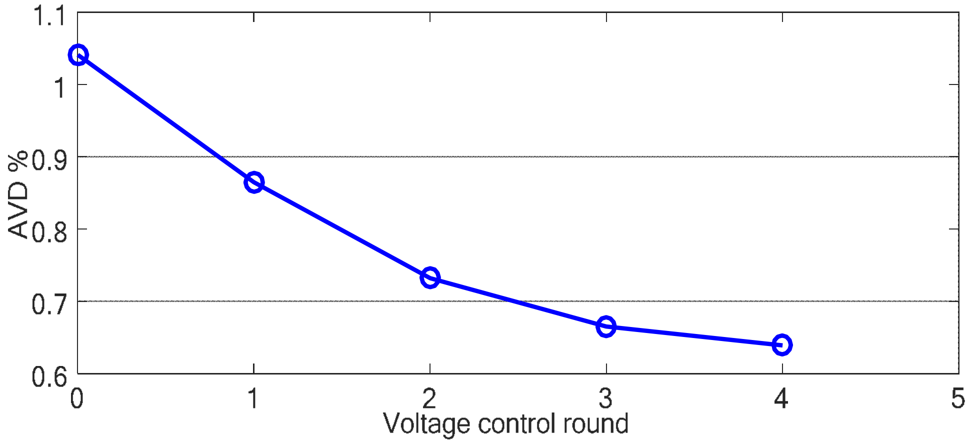

Figure 3-10 Average voltage deviation from the target voltages in consecutive rounds of control, objective: loss minimisation.

3.3.2 Application of the Proposed Multi-Objective AVM

For a week-long period, the active and reactive demands and other required data have been extracted for this system. These data can be found in **D3.3**. VVCs are extracted for the multi-objective case where two important objectives from the system operator's point of view, i.e., voltage unbalance minimisation as the first objective and active power loss minimisation as the second objective are considered to be improved simultaneously. This framework enables the system operator to consider any different (and probably opposing objectives) simultaneously.

The potential of incorporating V2G systems, i.e., the batteries of EVs and inverters of the charging stations (with bidirectional reactive power exchange capability) is investigated in the low voltage distribution network introduced in this subsection. As mentioned before, it has been assumed that the system operator is interested in simultaneous minimisation of the voltage unbalance at all the load points and energy loss to increase the power quality of the low voltage consumers connected to this test system and to reduce the system cost, respectively.

As explained in **D3.3**, in the first step the optimal voltage levels should be found for all V2G inverters. These voltages are referred to as the target voltages and in this subsection, the inverters should follow these voltages to simultaneously minimise the voltage unbalance index and power loss. The second stage in the offline calculations determines the optimal reactive power injections of V2G systems in each scenario that lead to the closest voltage levels to those obtained for V2G inverters in the first stage. The second stage in the offline calculations considers the capacity constraint as the only limitation on the operation of the V2G systems connected to this sample system. In order to analyse the effectiveness of the proposed voltage management algorithm, the actual limitations of these systems are taken into account when these VVCs are applied to find the reactive power injection of each inverter in the online studies.

In Stage 3, the voltages of all inverters are found in each scenario considering no reactive power injection for the network inverters. The VVCs are extracted by applying a linear regression technique on all the (voltage)-(reactive power injection) pairs found in the third and second stages, respectively. For more discussion see **D3.2** and **D3.3**. Fehler! Verweisquelle konnte nicht gefunden werden.**Table 3-3** gives the results of the offline studies producing the following characteristics for the V2G connections under examination. Parameters of the VVCs (*m* and *c*) and also the target voltages are given in this table.

As discussed in **D3.3**, active voltage management include different control modes for the inverter-based resources to optimise performance depending on whether the generator is connected to the grid, or in island mode. Therefore, they can be set to maintain the voltage (voltage control mode), the PF (power factor control mode) or the reactive power (power control mode). Here, we assume that the inverters can be operated in both power control mode and voltage control modes of operation.

In the online simulations of this subsection, the extracted VVCs (see **Table 3-3**) are applied to find the optimal reactive support of the inverters of this sample system in power control mode of operation. It should be noted that the target voltages reported in **Table 3-3** can be considered as the voltage set-points in the voltage control mode of operation for these controllable devices.

If the inverters follow these target voltage set-points in the voltage control mode of operation, the results will be the same as those that are obtained in power control model of operation where the inverters are tasked with following the reactive power levels that are found using the VVCs. In other words, in both control modes, the controllable devices should try to follow the optimal voltages as accurate as possible considering the operational limitations which depend on the type of the controllable devices connected to the system. These limitations were introduced in **D3.3** for different types of RESs.

Table 3-3 Optimal inverter voltages (for voltage control mode), slope and intercept of V2G systems for power control mode. Objective: Multi-objective (Simultaneous minimisation of loss and voltage unbalance)

V2G system	Power control mode of operation			Voltage control mode of operation	Relative Error %
	m (pu/kVAR)	c (pu)	Reactive power control equation $\Delta Q=\alpha . V_{pcc}+\beta$	V_{opt} (pu)	
1	-0.00057	0.98373	$\Delta Q= -1752.1544V_{pcc}+ 1723.6444$	0.9847	0.0971
2	-0.00884	0.98499	$\Delta Q= -113.1492V_{pcc}+ 111.4510$	0.9853	0.0360
3	-0.01007	0.98033	$\Delta Q= -99.2938V_{pcc}+ 97.3407$	0.9802	0.0103
4	-0.00810	0.98042	$\Delta Q= -123.4866V_{pcc}+ 121.0683$	0.9816	0.1228
5	-0.01549	0.97520	$\Delta Q= -64.5687V_{pcc}+ 62.9674$	0.9762	0.0974
6	-0.00897	0.98110	$\Delta Q= -111.4642V_{pcc}+ 109.3574$	0.9825	0.1426
7	-0.00817	0.97606	$\Delta Q= -122.3467V_{pcc}+ 119.4177$	0.9764	0.0374
8	-0.01750	0.97501	$\Delta Q= -57.1446V_{pcc}+ 55.7168$	0.9761	0.1157
9	-0.01158	0.97876	$\Delta Q= -86.3402V_{pcc}+ 84.5063$	0.9802	0.1493

All the slopes of the VVCs are negative. This leads to a positive reactive power injection when the measured voltages at PCCs are below the regarding target voltages (V_{opt}) and a negative reactive power injection (positive absorption) when the measured voltages are higher than the target voltages presented in **Table 3-3**.

This validates the successful application of the proposed AVM algorithm. This is as expected as, under stable operation (static voltage control), an injection of reactive power at the connecting bus of a controllable inverter increases the voltage magnitude at this location and a reactive power absorption at this node reduces this voltage.

The intercept *c*, closely matches the optimal voltage (V_{opt}). This indicates the effectiveness of the proposed method for active voltage management based on VVCs and validates application of the optimal voltages (V_{opt}) as the voltage set-points of the system inverters in the voltage control mode of operation as explained in **D3.3**. The relative error is presented in **Table 3-3** for each V2G system. The VVCs of all 9 V2G systems are presented in **Figure 3-11**.

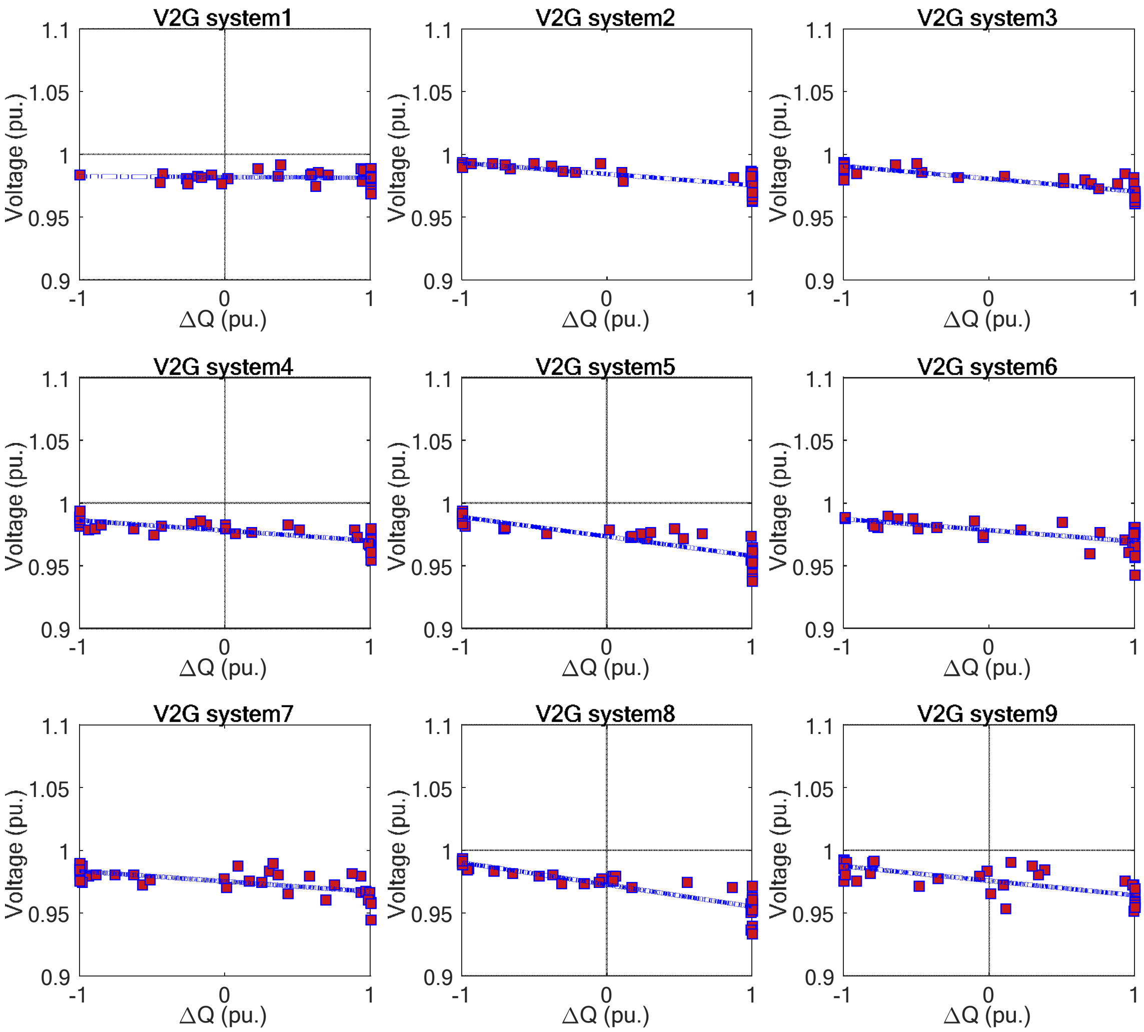

Figure 3-11 Resulting VVCs found for the simultaneous minimisation of the power loss and voltage unbalance for V2G systems 1-9, showing intercepts and slopes

Similar to D3.3, in order to validate the ability of the adopted 3-phase power flow algorithm to converge to a stable solution while there are many controllable devices connected to the low voltage distribution system under study, and also to assess the voltage controllability of the inverters, the three-phase voltages are presented in **Figure 3-12**. The voltage of each inverter is fixed on the values presented for target voltages in the multi-objective study.

Figure 3-13 presents the value of the reactive power that each inverter should supply at PCC. Some of these reactive power injection values are negative, signifying reactive power consumption by these inverters. No active power injection/consumption is allowed by these V2G systems in the calculation of the reactive power injections presented in **Figure 3-13**. This means all the capacity of each inverter can be dedicated to reactive power support. The active and reactive power demands at all load points and other load characteristics have been set to the values regarding the most probable scenario. See **D3.3** for more information and observations.

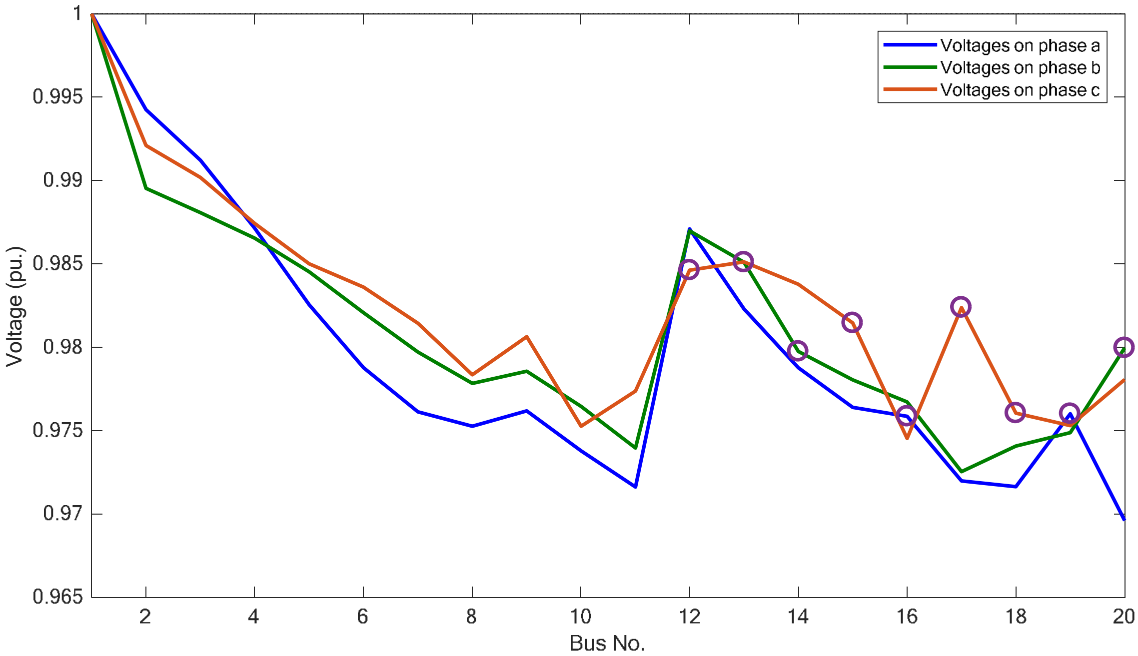

Figure 3-12 Voltage levels at different system buses, buses 12-20 are the PCCs of the V2G systems (Multi-objective)

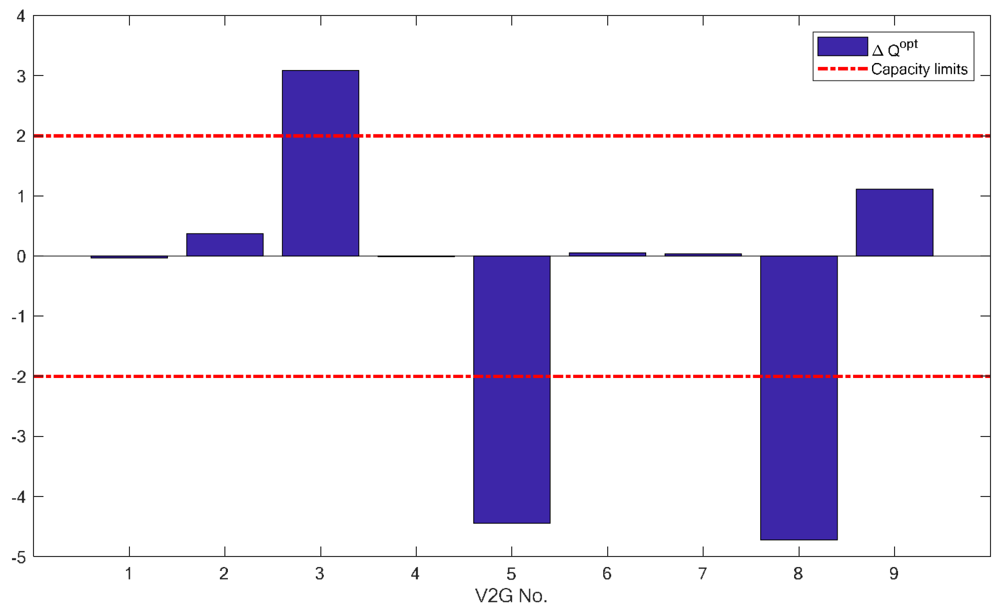

Figure 3-13 Reactive power injection of each V2G inverter in order to achieve the target voltage levels for each inverter (Multi-objective)

In order to show how the proposed multi-objective framework makes a compromise between the first and second objectives in this study, Figure 3-14 presents the average values of the voltage unbalance at different load points (buses 2-11) of this sample system. As can be seen, with the multi-objective framework, the value of the average voltage unbalance at most of the load points is between the values of this parameter for the first and the second objectives, i.e., minimisation of the voltage unbalance and loss minimisation.

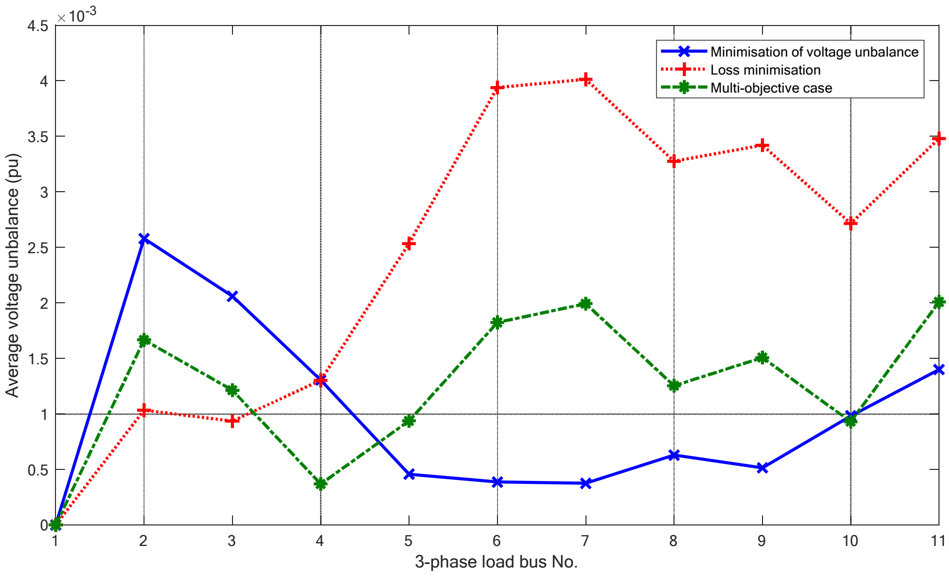

Figure 3-14 Average voltage unbalance at 3-phase load buses with different objectives (Minimisation of Voltage Unbalance, Loss Minimisation, Multi-objective)

To validate the effectiveness of the proposed multi-objective active voltage management framework, the minute by minute active and reactive power demands at all load points and also the other required data are considered to be similar to those assumed for validation of the proposed single objective AVM algorithm in **D3.3**. This enables us to compare the results of the single and multi-objective AVM algorithm. In a week-long period, the V2G systems on this LV feeder are tasked with following their assigned VVCs found using the multi-objective AVM algorithm, i.e., the VVCs presented in Figure **3-13**.

In three separate studies, the three different fixed power factor operation strategies are assumed for the V2G systems connected to this low voltage distribution system, i.e., 0.95 inductive, 1 and 0.95 capacitive. These settings constrain the reactive power support of each V2G inverter to absorb roughly one-third of the value of active power consumed by the V2G charger, zero and inject about one-third of the value of active power consumed by the V2G charger. A fixed power factor is typical for an inverter based controllable device connected to a low voltage distribution system to reduce the voltage-rise effect caused by the excessive active power injections. The operation of the set-points extracted using the VVCs are compared to the operation at the aforementioned fixed power factor strategies.

The effects of different constraints on the effectiveness of the multi-objective framework are also investigated. Similar to **D3.3**, the results are also compared to those obtained with the case that the capacity constraints are considered as the only constraints and also the results of the fixed power factor criteria. The observed voltage measurement at the terminals of the V2G systems are mapped to their set-point operation of reactive power using 9 different studies.

More information regarding the week-long validation of the local voltage control algorithm can be found in **D3.3**. Here, the main focus is on analyzing the results of multi-objective AVM algorithm. As mentioned in **D3.3**, the values gained for the average voltage unbalance and weekly energy loss considering the minimisation of the average voltage unbalance and loss minimisation in Table 3-4 suggests that there may be some strategies that can reduce the voltage unbalance and energy loss simultaneously. Here, this strategy is found using the proposed multi-objective framework.

According to the results provided in Table 3-4 for multi-objective framework, we can analyse how the sets of constraints considered for the operation of the inverter-based controllable devices can affect the performance of the proposed AVM algorithm. With the accurate constraint modelling (see the simulation results provided in **D3.3**), the results of applying the proposed AVM algorithm for optimising the reactive power dispatch to simultaneously minimise the voltage unbalance and power loss are even better than those obtained for the case with capacity constraint as the only constraint on the operation of the system inverters. For the single objective studies, the same phenomenon is observed. The reasons were discussed in **D3.3**.

For the case study with a maximum lagging power factor of 0.92, the proposed multi-objective AVM algorithm leads to a total loss and voltages unbalance lower than the best energy loss and voltage unbalance attained with the fixed power factor assumption. This shows the efficiency of the proposed active voltage management algorithm even with such restricted feasible area is considered for the reactive power injection of the system inverters.

The more important point that should be noted is that in all studies presented in Table 3-4, for multi-objective case, the value of the voltage unbalance is better than the voltage unbalance found for the regarding single objective loss minimisation study. However, this voltage unbalance is not lower than the one obtained for the regarding single objective minimisation of the voltage unbalance. For the weekly energy loss, the results of the multi objective algorithm is better than those obtained for the single objective minimisation of the voltage unbalance but not as optimal as those obtained for the single objective loss minimisation case. Multi-objective framework leads to an energy loss 6.61% lower than the energy loss found for the single objective minimisation of the voltage unbalance, but only 0.61% higher than the loss found for the single objective minimisation of the power loss. The value of the voltage unbalance is 23.5% lower for multi objective framework comparing to the voltage unbalance obtained with single objective loss minimisation while with the multi-objective framework the value of this value is only 5.94% higher than the one obtained for single objective minimisation of the voltage unbalance. This indicates the acceptable efficiency of the proposed multi-objective decentralized active voltage management.

The effects of different constraints on the PQ capability curve and also the active and reactive power injections of all the inverters in multi-objective case are presented in **Figure 3-15**.

Table 3-4 Comparison of active power loss and voltage metrics

Objective	Total Energy Loss (kWh)	Average Voltage Unbalance
Min. Voltage Unbalance	313.4432	0.012584
Min. V. Unbalance with accurate operational constraints	303.5436	**0.012124**
Min. Voltage Unbalance Available NC Recommendation, Lagging PF>0.92	297.6478	0.015234
Min. Power Loss [kW]	283.9466	0.015801
Min. Power Loss with accurate operational constraints	**282.9815**	0.015244
Min. Power Loss [kW] NC recommendation Lagging PF>0.92	290.4841	0.015918
Multi-objective	297.4471	0.013176
Multi-objective with accurate operational constraints	**284.7254**	**0.012890**
Multi-objective [kW] NC recommendation Lagging PF>0.92	293.2985	0.015334

Fixed Power Factor	0.95 Lag Power factor	297.1450	0.017371
	Unity Power factor	298.9494	0.017235
	0.95 Lead Power factor	301.1108	0.017186

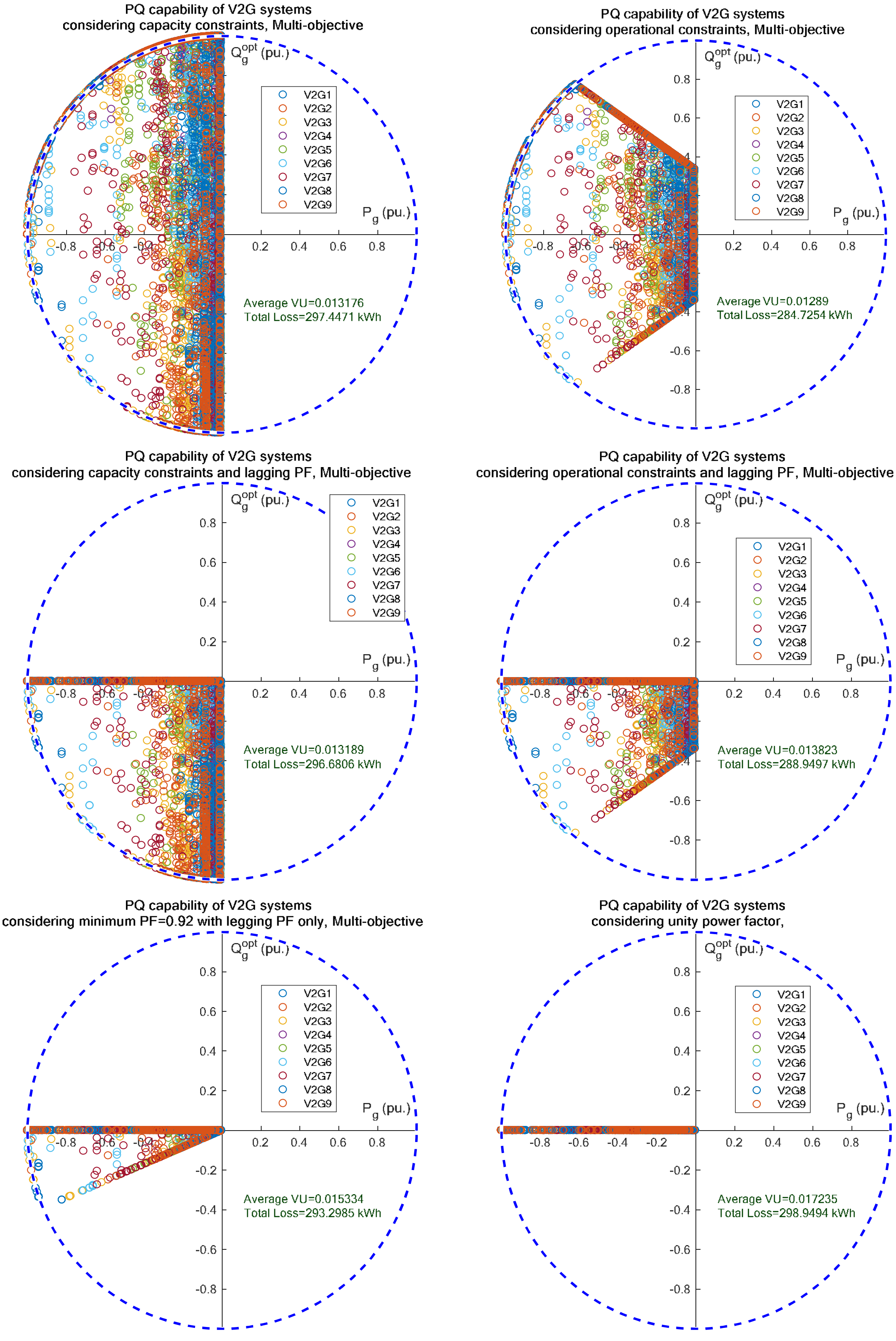

Figure 3-15 Active and reactive power capability curves, Multi-objective optimisation for simultaneous minimisation of the total energy loss and average voltage unbalance.

3.4 Active Voltage Management – Volt var curve execution

The execution of the Volt-var Curve (VVC) involves the receipt of the VVC, the storage of the VVC and the calculation of Reactive Power (Q) based on the VVC and the voltage readings (v) sent up from a DER Unit. The software application that carries out this execution is built in a modular way to reflect the centralised, decentralised and hybrid architecture models defined in D3.6 section 3.1.2. This means that the components charged with the receipt, storage and execution of the VVC, while inter-dependant, can be individually deployed in various locations throughout the system.

The execution of the VVC comprises of 3 base components, a VVC management service, a VVC storage service and a VVC execution service.

The **VVC Management Service** is a service that handles the upload of new VVC's and the updating, reading and removal of pre-existing VVC objects. This is a web based Representational State Transfer (REST) enabled service which is deployed on a cloud central server that provides a single access point to upload VVCs, thus helping to reduce security concerns and eliminate the need for multiple interface management for each DER Unit.

The **VVC Storage Service** is a database that is run in a central cloud server that stores the VVC objects for all sites. Of note in a Hybrid Architecture there will be another database running independently which will store Volt-var Curves for the sites it is responsible for. Each VVC stored has reference to its specific RES Unit via a unique identifier, this assists with the retrieval of the VVC for execution or deployment to its designated DER Unit.

The **VVC Execution Service** has three basic functions, the receipt of the voltage values from the RES Unit, the calculation of the Set Point Value based on the voltage received and the VVC, and the sending of the Set Point to the DER Unit.

The receipt of the voltage values from the DER Unit and the sending of the set point to the DER Unit is carried out using MQTT. The MQTT message broker system adopts the publish/subscribe communication model. This means that when a message is published to a certain channel, anything subscribed to that same channel will receive the payload. The channels themselves are unique to each MQTT message broker, so a publisher and subscriber must be connected to the same message broker to communicate. The payloads sent on these channels are also expected to be in a JSON format as it is much more lightweight than a standard XML format and is more manageable than a binary format.

The calculation of the setpoint value is carried out using an algorithm that derives Reactive Power (Q) from the VVC and the normalised voltage received from the DER Unit. This calculated using the formula $Q = v - c / m$ with the value c represents the intersection point of the VVC and m represents the slope and v value representing the normalised form of the voltage reading that is received from the DER Unit. There is a requirement to ensure that setpoint values are kept within a range between -1 and 1. If the initial calculation is found to be below -1 then it is defaulted to -1, similarly if it is found to be above 1 then setpoint value is defaulted to 1.

The execution of the algorithm can be deployed at different locations such as a central cloud server, a regional mobile edge computing site or an edge device on or at the DER Unit to suit the requirements of either the Centralised, Hybrid or Decentralised architectures detailed in D3.6.

3.5 ICT Infrastructure for AVM

The execution of the AVM algorithm and more accurately the Volt-var Curve (VVC), which is the actionable output from the algorithm, from an ICT perspective, involves the implementation of a set of suitable architectures/approaches that will allow an effective execution from both a simulation and trial site implementation. With reference to D1.3 section 2.3 the author refers to centralised, decentralised and distributed approaches from an electrical engineering perspective but to fully explore the potential execution of the AVM we must discuss these architectures in terms of an information technology, distributed systems approach. This approach has its foundation in communications and networking and comprises of the interconnection of heterogeneous physical and virtual components distributed across a local area network (LAN) or wide area network (WAN) for data transfer and system control. There are three architectural models detailed in D3.6 section 3.1.2, a Centralised model, a Decentralised model and a Hybrid

Edge Computing model, from the perspective of their mechanics, topological structure and high-level ICT requirements. The main differences between each architecture are in terms of the geographical distance between the execution of the VVC and the inverter and the autonomy of each RES unit from a central control point in terms of voltage management and the granularity of control. From a trial site perspective, there are components that facilitate this execution from a hardware and communications aspect. Each trial site is different in terms of ICT infrastructure and this is driven by such factors as RES Inverter capability, level of access to the RES Device and available interfaces on the RES Unit for communications. Full details of the trial site specifics can be found in D5.2.

4. Reporting of Field Trial Activities

4.1 Overview

Field trials for the testing of the Voltage Control concepts developed within the RESERVE are being progressed in Ireland. The trials seek to robustly test the performance of these voltage control techniques in some complex real-world environments in which the trials will build on the extensive simulation work undertaken to date. The field trial installations have been designed to collate the relevant system parameters, both local to the device and at remote locations on the feeder, to assess and quantify the control technique’s impact. Feedback of this performance data will also allow for further refinement of the control techniques for them to provide more substantive impacts.

4.2 Field Trial Technologies

The field trials constitute a mix of inverter-based technologies which are currently experiencing significant growth in deployment globally, these include;

- Solar Photovoltaic (PV) Systems
- Vehicle to Grid (V2G) Charging Systems
- Domestic Battery Storage Systems

In addition to the trialling of new voltage control techniques using these established technologies, the field trials will also see the first operational deployment of a newly designed and developed prototype inverter. This inverter developed by RWTH Aachen will allow for trialling of the VOI based control technique, detailed previously, at a 38 kV distribution station in Portlaoise, Ireland.

4.3 Additional Detail

Significant additional detail on the Field Trial Activities is documented in Deliverable **D5.2**.

5. Conclusion

This deliverable concludes ***T3.5 System level Monitoring Concept***. This deliverable defines and specifies the system level monitoring concept for the two voltage scenarios: Dynamic Voltage Stability Monitoring (DVSM) and Active Voltage Management (AVM). The milestone **MS 8** which is on the definition and specification of system level monitoring concept was achieved by the completion of Task **T3.5**.

DVSM is defined as a three-step process where the DSO operator in SSAU controls the inverters through 5G ICT infrastructure. The last step of the DVSM is the Virtual Output Impedance (VOI) synthesis and a novel technique for VOI synthesis is proposed in this deliverable.

A gap was identified in the way VOI controllers were defined. Many of the methods do not take the time-varying nature of the grid impedance. Few of the methods that do consider grid impedance measurement do not have a generalised design procedure for the design of VOI controllers. This deliverable addresses the above-mentioned gap by presenting a generalised framework for the synthesis of a class of robust VOI controllers based on the real-time grid impedance measurements. Parameters of the weighting function can be used to modify the inverter output impedance. Validation of the proposed technique is performed in both time and frequency domain in offline simulations.

System level implementation of the SV_A technique was analysed. Particularly, the placement of the WSI tool in the system. The first possibility is the inverter hosting the WSI tool locally. The controller hardware needs to be computationally powerful whereas the communication data volume is low. The second possibility is where the WSI tool is implemented centrally in SSAU. Here, the data volume is high although the controller of the inverter can be cheap.

In **D3.2** to **D3.4**, a decentralized AVM technique was developed based on VVCs extracted using the offline simulations. By applying VVCs to find the new settings of the system flexible devices, it is possible that more corrections are required, since the PCC voltages may not be equal to the target voltages proposed by VVCs. A supervised closed-loop control was proposed in Chapter 3 to achieve a near optimal voltage management scheme. The other tasks of the system level control is to initiate the control process to reach a balanced state. The results of the regarding case studies show the effectiveness of the proposed supervised system level control in achieving a stable high-quality solution in a few iterations. It is noticeable that in this hybrid control framework the control strategies are still extracted by the local control systems in a short period to meet the real-time requirements of AVM in the current distribution systems.

It was also shown in the case studied that for the LV distribution systems with high penetration level of controllable devices, the load point voltages can be managed more effectively to exploit all the control capacity available. The active voltage management algorithm proposed in **D3.2** and **D3.3** was extended to satisfy more than one objectives at the same time. In the case studies minimization of the voltage unbalance and loss minimization were considered simultaneously. The results showed that both voltage unbalance and system loss are significantly improved while the objective functions of the single-objective problems were just slightly increased. This shows the effectiveness of the proposed multi-objective framework.

5.1 Future Work

Simulations/Field trials are mapped with network codes proposed in WP3. In last year of the project, the validation of the concept and network codes will be carried out and reported in *D3.8* and *D3.9.*

6. List of Figures

7. List of Tables

8. References

[1] C. Yoon, H. Bai, R. N. Beres, X. Wang, C. L. Bak, and F. Blabjerg, “Harmonic Stability Assessment for Multiparalleled, Grid-Connected Inverters,” vol. 7, no. 4, pp. 1388–1397, 2016.

[2] J. Sun, “Impedance-Based Stability Criterion for Grid-Connected Inverters,” *IEEE Trans. Power Electron.*, vol. 26, no. 11, pp. 3075–3078, 2011.

[3] Y. Xu, L. Guan, Z. Y. Dong, and K. P. Wong, “Transient stability assessment on China Southern Power Grid system with an improved pattern discovery-based method,” in *Power System Technology (POWERCON), 2010 International Conference on*, 2010, pp. 1–6.

[4] T. S. A. Aapro, T. Messo, T. Roinila, “Effect of active damping on output impedance of three-phase grid-connected converter,” *IEEE Trans. Ind. Electron*, vol. 64, no. 9, pp. 7532–7541.

[5] H. W. D. Yang, X. Ruan, “Impedance shaping of grid-connected inverter with lcl filter to improve its adaptability to weak grid Condition,” *IEEE Trans. Power Electron*, vol. 29, no. 11, pp. 5795–5805.

[6] X. Wang, F. Blaabjerg, and P. C. Loh, “Passivity-Based Stability Analysis and Damping Injection for Multiparalleled VSCs with LCL Filters,” vol. 32, no. 11, pp. 8922–8935, 2017.

[7] L. P. Z. Chen, X. Pei, M. Yang, “An adaptive virtual resistor (avr) control strategy for low-voltage parallel inverters,” *IEEE Trans. Power Electron*, 2018.

[8] M. Cespedes and J. Sun, “Adaptive control of grid-connected inverters based on online grid impedance measurements,” *IEEE Trans. Sustain. Energy*, vol. 5, no. 2, pp. 516–523.

[9] W. W. Y He, H. S. hung Chung, C tak Lai, X Zhang, “Active cancellation of equivalent grid impedance for improving stability and injected power quality of grid connected converter under variable grid condition,” *IEEE Trans. Power Electron*, 2018.

[10] A. Riccobono and A. Monti, “Noninvasive Online Parametric Identification of Three-Phase AC Power Impedances to Assess the Stability of Grid-Tied Power Electronic Inverters in LV Networks,” *IEEE J. Emerg. Sel. Top. Power Electron.*, vol. 6, no. 2, pp. 629–647.

[11] B. Wen, D. Boroyevich, R. Burgos, P. Mattaveli, and Z. Shen, “Analysis of D-Q Small-Signal Impedance of Grid-Tied Inverters,” *IEEE Trans. Power Electron.*, vol. 31, no. 1, pp. 675–687, 2016.

[12] B. Wen, D. Boroyevich, R. Burgos, P. Mattaveli, and Z. Shen, “Inverse Nyquist Stability Criterion for Grid-Tied Inverters,” vol. 32, no. 2, pp. 1548–1556, 2017.

[13] C. Desoer and Y.-T. Wang, “On the generalized nyquist stability criterion,” vol. 25, no. 2, pp. 187–196, 1980.

[14] A. G. J. MacFarlane and I. Postlethwaite, “The generalized Nyquist stability criterion and multivariable root loci,” vol. 25, pp. 81–127, 1977.

[15] S. Skogestad and I. Postlethwaite, *Multivariable Feedback Control - Analysis and Design*. .

[16] L. Abdullah, “Fuzzy Multi Criteria Decision Making and its Applications: A Brief Review of Category,” *Procedia - Soc. Behav. Sci.*, 2013.

[17] C. Kahraman, “Multi-Criteria Decision Making,” *Fuzzy Multi-Criteria Decis. Mak.*, 2008.

[18] P. Richardson, D. Flynn, and A. Keane, “Local Versus Centralized Charging Strategies for Electric Vehicles in Low Voltage Distribution Systems,” *Smart Grid, IEEE Transactions on*, vol. 3, no. 2. pp. 1020–1028, 2012.

[19] A. O’Connell, “Unbalanced distribution system voltage optimisation,” in *PES Innovative Smart Grid Technologies Conference Europe (ISGT-Europe), 2016 IEEE*, 2016, pp. 1–6.

[20] A. O’Connell, D. Flynn, and A. Keane, “Rolling Multi-Period Optimization to Control Electric Vehicle Charging in Distribution Networks,” *IEEE Trans. Power Syst.*, vol. 29, no. 1, pp. 340–348, Jan. 2014.

[21] M. Bakhtvar and A. Keane, “A study of operation strategy of small scale heat storage devices in residential distribution feeders,” in *PES Innovative Smart Grid Technologies Conference Europe (ISGT-Europe), 2017 IEEE*, 2017, pp. 1–6.

9. List of Abbreviations

AC	Alternating Current
ADMD	After Diversity Maximum Demand
AFCI	Arc Fault Circuit Interrupter
ASHP	Air-Source Heat-Pump
AVM	Active Voltage Management
B2B	Business to Business
BMS	Building management system
BST	Battery Storage Technology
CAPEX	CAPital Expenditure
CCM	Component Connection Method
CENELEC	European Committee for Electro technical Standardization
CEP	Complex Event Processing
COTS	Commercial off-the-shelf
CPMS	Charge Point Management System
CPL	Constant Power Load
CPS	Constant Power Source
CSA	Cloud Security Alliance
EMS	Decentralised energy management system
DC	Direct Current
DER	Distributed Energy Resources
DG	Distributed Generator
DMS	Distribution Management System
DMTF	Distributed Management Taskforce
DSE	Domain Specific Enabler
DVSM	Dynamic Voltage Stability Monitoring
EAC	Exploitation Activities Coordinator
ERP	Enterprise Resource Planning
ESB	Electricity Supply Board
ESAC	Energy Source Analysis Consortium
ESCO	Energy Service Companies
ESO	European Standardisation Organisations
ETP	European Technology Platform
ETSI	European Telecommunications Standards Institute
EV	Electric Vehicle
GE	Generic Enabler
GM	Gain Margin
GMPM	Gain Margin Phase Margin
GNC	Generalised Nyquist Criterion
HEMS	Home Energy Management System
HV	High Voltage
I2ND	Interfaces to the Network and Devices
ICT	Information and Communication Technology
IEC	International Electro-technical Commission
IGDT	Information Gap Decision Theory
IoT	Internet of Things
KPI	Key Performance Indicator
LRC	Line Regulated Converter
LV	Low Voltage
LVAC	Low Voltage AC
MIMO	Multiple Input Multiple Output
MLG	Minor Loop Gain
M2M	Machine to Machine
MPLS	Multiprotocol Label Switching
MPP	Maximum Power Tracking
MV	Medium Voltage
NIST	National Institute of Standards and Technology
O&M	Operations and maintenance
OLTC	On Load Tap Changer
OPEX	OPerational Expenditure

OPF	Optimal Power Flow
PBSC	Passivity Based Stability Criterion
PCC	Point of Common Coupling
PLL	Phase Locked Loop
PM	Phase Margin
PMT	Project Management Team
POL	Point of Load
PPP	Public Private Partnership
PRBS	Pseudo Random Binary Sequence
PV	Photovoltaic
QEG	Quality Evaluation Group
RES	Renewable Energy System
RHP	Right Half Plane
RMS	Root Mean Square
S3C	Service Capacity; Capability; Connectivity
SCADA	Supervisory Control and Data Acquisition
SDH	Synchronous Digital Hierarchy
SDN	Software Defined Networks
SDOs	Standards Development Organisations
SET	Strategic Energy Technology
SET	Strategic Energy Technology
SG-CG	Smart Grid Coordination Group
SGSG	Smart Grid Stakeholders Group
SME	Small & Medium Enterprise
SoA	State of the Art
SON	Self Organizing Network
SRF	Synchronous Reference Frame
SS	Secondary Substation
SSAU	Secondary Substation Automation Unit
TL	Task Leader
TM	Technical Manager
UL	Underwriters Laboratories
VOI	Virtual Output Impedance
VPP	Virtual Power Plant
WP	Work Package
WPL	Work Package Leader
WSI	Wideband System Identification
ZIP	constant impedance Z, constant current I, and constant power

Annex

A.1 Fuzzy multi-objective decision making

Multiple criteria decision making (MCDM) is a modelling and methodological tool for dealing with complex engineering problems involving different and sometimes opposing objectives. Decision makers face many problems with incomplete and vague information in MCDM problems since the characteristics of these problems often require this kind of information. Fuzzy set approaches are suitable to use when the modelling of human knowledge is necessary and when human evaluations are needed. Fuzzy set theory is recognized as an important problem modelling and solution technique. Fuzzy set theory has been studied extensively over the past 40 years. Most of the early interest in fuzzy set theory pertained to representing uncertainty in human cognitive processes. Fuzzy set theory is now applied to problems in engineering, business, medical and related health sciences, and the natural sciences. Over the years there have been successful applications and implementations of fuzzy set theory in MCDM. MCDM is one of the branches in which fuzzy set theory found a wide application area.

Outranking methods form one of the main families of methods in multiple criteria decision aid (MCDA). The outranking methods are based on the construction and the exploitation of an outranking relation. The underlying idea consists of accepting a result less rich than the one yielded by multi-attribute utility theory by avoiding the introduction of mathematical hypotheses that are too strong and asking the decision maker some questions that are too intricate.

In contrast to the other methods, the outranking methods have the characteristic of allowing incomparability between alternatives. This characteristic is important in situations where some alternatives cannot be compared for one or another reason. Incomparability between two alternatives can occur because of a lack of information, inability of the decision maker to compare the two alternatives, or his refusal to compare them.

In fuzzy domain, each objective is associated with a membership function. The membership function indicates the degree of satisfaction of the objective. In the crisp domain, either the objective is satisfied or it is violated, implying membership values of unity and zero, respectively. When there are multiple objectives to be satisfied simultaneously, a compromise has to be made to get the best solution.

In fuzzy domain, the degree of satisfaction of each objective is specified by a value between 0 and 1 (signifying the worst and best possible objective function values). For each objective, it is necessary to find the best and worst values of objective function considering all the constraints regarding to this objective and all the options available for satisfying the objective. A single-objective optimisation should be conducted to find the optimal set-points of the network inverters to minimise the voltage unbalance as the first objective (Obj_1) satisfying all the problem constraints. This optimisation gives the value of Obj_1^{min}, which is the best value that can be achieved for this objective, assuming there is no other objectives to be taken into account.

In order to find the worst value of this objective function (Obj_1^{max}), one approach (which is used here) is to find the value of this objective function without applying any reactive power support.

Fig. 1 shows the membership function of the first objective. As can be seen the degree of satisfaction of the first objective increases monotonically as the value of this objective function decreases from Obj_1^{max} to Obj_1^{min}.

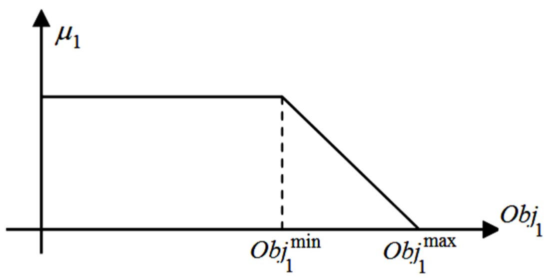

Figure A-1: Membership function of the first objective.

The best and worst values of the other objective functions should be found in the same way, in order to build the membership function of these objectives. The details of applying this membership functions to satisfy all the objectives simultaneously is presented below.

Each solution vector contains the value of the reactive power injection of all the network inverters. For each solution vector (individual) X, the values of Obj_1 and Obj_2 are calculated according to the explanations provided in deliverable D3.2. The values of membership functions of voltage unbalance and voltage deviation problems ($\mu_1(X)$ and $\mu_2(X)$) are found next. The final fitness function is provided in (1). The optimisation tries to maximize this fitness function. In this way, the multi-objective problem is converted into a single objective one which can be solved using any desired optimisation technique which is applicable to this problem. The penalty function p_i is defined in (2). In this formulation W is a very large constant. Since there is an upper bound for $\mu_1+\mu_2$, i.e. $\mu_1+\mu_2<2$, the value of this constant (W) can be set to reach the acceptable accuracy of constraints' satisfaction. The proposed method for finding the value of W coefficients will be discussed later. The following discussion explains application of the penalty functions for satisfying the decision maker constraints on the value of the problem objective functions.

The membership functions should increase monotonically from the worst value to the best value of the regarding objective functions. Selecting different shapes for the membership functions, gives different importance to the problem objectives. In this project the membership values change linearly between best and worst values of the regarding objective functions. In order to define a more controllable significance level for each objective, after defining the membership functions, the decision-maker is asked to specify the achievement degree of each membership function, i.e., reference membership function μ_{ref}, which takes the real values between 0 and 1. Higher values of this parameter show more importance, and hence give more weight to the regarding objective. The values of 0 and 1 for $\mu_{ref,i}$ show that the ith objective has the least and most importance for the decision-maker, respectively. This interactive fuzzy optimisation approach provides the optimal solution satisfactorily close to the decision-maker's requirements [33].

Sometimes, the satisfaction levels of some objectives need to be higher than the specific values. In fuzzy multi-objective optimisation, it is possible to consider such limitation. The decision maker can specify the minimum accepted values of each membership function. However, it may be not possible to satisfy these constraints. In this situations, these constraints can render the optimisation problem infeasible. Therefore, special cares should be taken in introduction of such constraints to the optimisation algorithm. The rest of this subsection explains how the decision maker can take the objectives' importance into account via adjusting the parameters μ_{ref}.

A brief discussion is provided here to show how the big constant coefficients in equation (2) should be found. As explained before, in order to satisfy the decision maker's constraints on the value of each membership function, the parameter free penalty function approach is used for constraint handling based on [27]. The fitness value of an infeasible solution depends on the amount of constraint violation. In this way, the objective function, i.e., $\mu_1+\mu_2$ and the penalty functions form the expended objective function (fitness value) which is provided in (1).

In the penalty functions, the values of the constraint violations are multiplied by big constants (M) to raise the value of objective function proportional to the constraint violation. This constraint violation handling scheme pushes the infeasible solutions towards the feasible region. In most of applications it is quite sufficient to consider the very large M constants. However, to select the big M constants that improve the convergence speed and solution optimality, three questions should be answered.

1. Which constraints are harder to be fulfilled?
2. Which constraint is more important in active voltage management?

3. What is the maximum acceptable Constraint Violation Tolerance (CVT)?

Among these parameters, selection of CVT is more important. Selecting a very low CVT may render the optimisation solution practically infeasible (due to pure satisfaction of the regarding constraints). On the other hand, selecting a very high CVT may cause sub-optimal solutions. To elaborate on the sides of the issue, it is noticeable that selecting a high CVT leads to a high value for the penalty function of the regarding constraint even for the infeasible solutions very close to the global optimum solution point. Such high value for the penalty function may push the search region of the optimisation algorithm away from the global optimum solution.

In some optimisation problems, an upper bound can be found for the objective function for the solutions with no constraint violation. In order to select the value of M constant for each constraint in such problems, it is sufficient that the regarding value of acceptable CVT is declared based on the constraint importance. It is obvious that selecting a higher M constant leads to lower CVT. This point is more discussed for the active voltage management problem introduced so far.

Since the value of each membership function μ_i is less than 1, an upper bound is found for the fuzzified objective function, i.e, $\mu_1+\mu_2$. This objective function is always less than 2. More accurately, the maximum value of fitness function with no constraint violation would be 2.

The value of objective function is bounded. Therefore, the value of each M constant can be found according to the declared acceptable CVTs, a simple comparison and operation practices. As an example, if the acceptable CVT for the first constraint (decision maker's constraints on the minimum value of the membership function for the first objective) is 0.001, it means that for a feasible optimisation problem, the violation of this constraint in the final solution should be lower than 0.001. In order to apply such restriction, as long as the constraint violation is higher than 0.001 in the process of search for the best solution, the penalty function of this constraint should be higher than the value of objective function ($\mu_1+\mu_2$). This forces the optimisation algorithm to decrease the constraint violation even though this decreases the value of objective function. Since the value of objective function is bounded ($Obj^{max}=2$), it is sufficient to select M_1 so that the value of p_1 is higher than Obj^{max} for the constraint violation of 0.001 ($Obj^{max}>0.01*M_1$ or $M_1>100*Obj^{max}$). Under such setup, the decision maker can be sure that when the optimisation terminates and the optimal solution is found, the maximum violation of this constraint is less than 0.001 or there is no other way to reduce the value of this violation. Based on the value of Obj^{max} and the above explanation, the value of these constants are $100*Obj^{max}$ for all M constants (CVT<0.01).